INTERFACE

royalsocietypublishing.org/journal/rsif

Research

Cite this article: Kuchling F, Singh I, Daga M, Zec S, Kunen A, Levin M. 2025 Uncertainty minimization and pattern recognition in *Volvox carteri* and *V. aureus*. *J. R. Soc. Interface* **22**: 20240645.
https://doi.org/10.1098/rsif.2024.0645

Received: 17 September 2024
Accepted: 21 January 2025

Subject Category:
Life Sciences–Physics interface

Subject Areas:
biophysics, systems biology

Keywords:
Volvox, surprise, minimal cognition, diverse intelligence, algae

Author for correspondence:
Michael Levin
e-mail: Michael.Levin@tufts.edu

Electronic supplementary material is available online at https://doi.org/10.6084/m9.figshare.c.7681862.

THE ROYAL SOCIETY PUBLISHING

Uncertainty minimization and pattern recognition in *Volvox carteri* and *V. aureus*

Franz Kuchling, Isha Singh, Mridushi Daga, Susan Zec, Alexandra Kunen and Michael Levin

Allen Discovery Center, Tufts University, Medford, MA, USA

FK, 0000-0003-2339-1991; ML, 0000-0001-7292-8084

The field of diverse intelligence explores the capacity of systems without complex brains to dynamically engage with changing environments, seeking fundamental principles of cognition and their evolutionary origins. However, there are many knowledge gaps around a general behavioural directive connecting aneural to neural organisms. This study tests predictions of the computational framework of active inference based on the free energy principle in neuroscience, applied to aneural biological processes. We demonstrate pattern recognition in the green algae *Volvox* using phototactic experiments with varied light pulse patterns, measuring their phototactic bias as a readout for their preferential ability to detect and adapt to one pattern over another. Results show *Volvox* adapt more readily to regular patterns than irregular ones and even exhibit memory properties, exhibiting a crucial component of basal intelligence. Pharmacological and electric shock-based interventions and photoadaptation simulations reveal how randomized stimuli interfere with normal photoadaptation through a structured dynamic interplay of colony rotation and calcium-mediated photoreceptor-to-flagellar information transfer, consistent with uncertainty minimization. The detection of functional uncertainty minimization in an aneural organism expands concepts like uncertainty minimization beyond neurons and provides insights and novel intervention tools applicable to other living systems, similar to early learning validations in simpler neural organisms.

1. Introduction

Living organisms are good at detecting, responding to and adapting to variable environments, not just on evolutionary time scales but also via short- and long-term adaptive organismal behaviour. Interestingly, this does not require brains or advanced nervous systems [1–4]. Examples of learning and adaptive behavioural responses in aneural organisms include context-dependent motility [5,6], stress response-triggered learning [7,8], anticipation [8], long-range spatial decision-making [9] and associative learning [10] in a range of microbial organisms. Even embryophytes, despite their apparent lack of dynamic motility, possess highly complex adaptive responses through their fast and complex internal calcium signalling patterns [11]. Similarly, in vascular plants, synaptic adhesion domains and action potentials [12,13] yield self-identity and recognition capabilities through their use of plant-specific synapses in *Cayratia japonica* [12], and can detect acoustic vibrations from feeding caterpillars and subsequent elicitation of chemical defences in *Arabidopsis thaliana* [14]. Furthermore, the slime mould *Physarum* detects material properties of its environment via pulsatile mechanosensing and makes growth decisions based on information gleaned about objects at long range [9]. In each of these examples, adaptation to environmental conditions occurs through a change of organismal behaviour, or, in a broader

sense, entering a different organismal or cellular active state. These adaptations range from changes of motility (direction and amplitude), physical properties such as chemical release (as a defence in plants), mechanical tension (which can regulate organismal shape or orientation, especially in plants), bioelectric state (modulated calcium signalling patterns), metabolic state (such as increased glucose consumption and biosurfactant production in response to ultrasonication in *Lactobacillus plantarum* [15]) to transcriptional changes leading to the expression of proteins that help the organism to deal with its new environment (such as heat shock proteins in high stress environments for example, and even cell identity changes in multi-cellular organisms).

The question at the heart of this study is what is the fundamental basis behind the emergence of these various modes of pattern detection that are so crucial to each form of basal cognition? Attempts to devise a unified framework for answering this question that complies with evolutionary theory and is supported by direct experimental evidence are missing. On the one hand, archaeological evidence as summarized by Peter Godfrey-Smith allows the recreation of a cognitive lineage in evolution as an arms race of action and detection [16] but falls short of providing a theoretical framework that explains its principal emergence. On the other hand, theoretical work by Terrance Deacon links goal-directed, 'teleodynamic' properties in biological organisms to the most basic forms of statistical physics [17], but fails to provide experimentally falsifiable predictions of cellular and organismal behaviour. Our work was hence motivated by two interrelated questions: how far down the evolutionary scale of complexity do organisms exhibit the ability to detect novel environmental patterns, and do they have expectations that may or may not be met? What frameworks can help us understand these capacities in novel substrates?

The ability to detect environmental patterns and distinguish them from random noise is considered a basic component of intelligence—the inference of a general pattern from particular experiences. Such a pattern can serve as the primitive basis of counterfactuals because the recognition of a pattern endows an organism with expectations for what should happen next before it happens. While ubiquitous seasonal and day–night cycles provide a highly reliable environmental pattern that is constant across generations (and thus can serve as a stable target for selection), it is unclear how much individual aneural organisms can detect and adapt to novel and more variable patterns on much shorter time scales.

Changes in a cell's extracellular environment can affect both its current physiological states and its future states, both physiological and genetic. An example of environmentally triggered immediate changes in current cellular active states is seen in basic phototactic organisms, where light-induced protein conformation states coupled with changes in flagellar beating rates result in movement towards or away from light stimuli. The short-term changes in light sensitivity and downstream flagellar beating responsivity that are the core of this ability to orient towards light and maintain direction are referred to as photoadaptation [18]. While the mechanisms of delayed adaptive responses of light-sensitive cells are fairly well understood in the human visual system as being mediated through intracellular signalling coupled to transcription, translation and epigenetic modifications, photoadaptation, especially in response to complex activation patterns, has not been well studied in simpler phototactic organisms such as *Volvox*.

Work over the last decade has shown that patterned environmental stimuli that differ only in the frequency of presentation to the organism can elicit distinct downstream signalling events and functional (behavioural) outcomes in many kinds of cellular systems. For example, pulsatile variation of osmotic concentrations leads to severe yeast growth inhibition as a result of frequency-specific activation and refractory relationship in the mitogen-activated protein kinase (MAPK) pathway, but only at specific frequencies of osmotic oscillation [19]. A similar phenomenon is presented by using optogenetics to dynamically activate signalling pathways [20], where optogenetic activation of epidermal growth factor (EGF) to vary the temporal dynamics of extracellular signal-regulated kinase (ERK) signalling leads to temporal variation in activation pulse frequency induction of ERK signalling that not only affects the amount of transcription and the subsequent translation of a target gene but can also trigger transcription of different target genes [21,22]. In *Volvox*, simple sinusoidal light stimulation patterns have been used to measure flagellar regulation [18], but not their effect on the overall colony behaviour and not in contrast to other types of activation patterns necessary to fully deduce complex organismal behaviour adaption.

Physiological bottom–up models employed in the examples above require a high degree of detailed knowledge of the underlying mechanistic biochemical pathway activation and require a high degree of experimental accessibility to those molecular pathways to be useful, which is not always possible. Thus, here we aimed to understand these phenomena from a top–down perspective focusing on the response of the system to patterns and information content in its environment—by generalizing a theoretical framework of adaptive responses to dynamic inputs reminiscent of higher level information processing common to many cellular systems. Using a cognitive Bayesian framework based on our earlier work [23] and that of Karl Friston and others in the field [24–29], we can formulate a model of cellular beliefs (or predictions) that encode what type of signals the cell expects to receive at any given point in time. These cellular beliefs encompass all the receptors and cellular machinery currently expressed and represent the cell's best estimate of which physiological and transcriptional state will make it the most adaptable to current and anticipated environmental effects [23,30]. Regulatory output aimed at modifying the signalling activity could hence be interpreted as the effort to minimize uncertainties in measurements of the environment compared with expected signalling inputs. Mechanistically, cellular expectations for input signalling activity stem from the state of the internal signalling pathway dynamics of the cell, itself encoded by transcriptional dynamics (with changes occurring in the range of minutes to hours) on the one hand, but also by more short-term state changes in protein conformations (e.g. opening and closing of ion channels and activation and internalization of receptor proteins) and activity profiles (ion inflow, propagation and available storage, such as encompassed through calcium dynamics) on the other. The ensuing transcriptional outputs and functional changes of proteins realize a constant modification of physiological and biophysical parameters affecting signalling transmission.

The uncertainty minimization employed by the cells as dictated by Bayesian inference [23] predicts that random (and hence unpredictable) dynamic stimulation will elicit a stronger but less directed cellular physiological and transcriptional response

than a regular, predictable dynamic stimulation, resulting in an aversion to irregular environments and preference for more regular ones [31]. Specifically, this idea has been developed in a rich body of work on surprise minimization [25,27,32–34], which emphasizes the drive of living beings to continuously improve their internal models of their environments and of themselves. These ideas are frequently discussed with respect to neural brain mechanisms; however, given the wide conservation of signalling mechanisms and algorithms across neural and non-neural cells [35,36], it becomes especially interesting to ask whether systems with no brains, and no neurons, can likewise support expectations about the future born of pattern inference and exhibit responses which reveal that these expectations cannot be met in random environments.

Here, we test the hypothesis that aneural organisms can display actionable pattern recognition in general and uncertainty minimization in particular. We chose to investigate this using the photoadaptive response in two different species of the chlorophyte green algae *Volvox* (*V. carteri* and *V. aureus*) as a readily measurable adaptive behaviour to an external physical stimulus that can be varied in any temporal pattern. We simulated different light stimulation patterns (including crucially randomized ones) in our model and tested their predictions for a variable effect on phototactic modulation in *V. carteri*. We designed an experimental platform that allows us to compare *Volvox* phototaxis towards two distinct regimes of light stimuli with different patterns of light pulsation, exploring mechanisms and long-term effects on the organism. We complement the phototactic trajectories obtained from these experiments with gain-of-function drug experiments focused on shifting phototactic biases based on both our knowledge of underlying molecular pathways and their effect on their information-processing modalities. We furthermore also tested whether *Volvox* exhibit short-term memory towards past light stimuli in terms of their phototactic paths, which would provide them with further crucial neural-like capabilities. We also tested whether *Volvox's* photosynthesis would also be affected by dynamic light patterns in an attempt to detect metabolic manifestations of uncertainty minimization in *Volvox*. Finally, to begin exploring the potential for training of *Volvox* phototaxis to desired light pattern biases, we examined whether patterned electric shocks could manipulate *Volvox* responses to patterned light stimuli. Taken together, our study aims to reveal capacities that would not normally be expected in algae and provide a proof-of-concept for searching for such capacities in a wide range of minimal and synthetic model systems that not only links existing theories of basal cognition to experimental evidence but crucially provides us with a testable behavioural directive of simple organisms and cells (uncertainty minimization) that can be applied to yield novel methods of intervention from medicine to ecology.

2. Methods

2.1. Culture conditions and strains

Volvox carteri eve strain (female) was obtained from Bradley J. S. C. Olsen Lab and grown in standard *Volvox* media (SVM), while *V. aureus* was obtained from Carolina (catalogue number 152655) and cultured exclusively in AlgaGro®. Both strains are incubated in a Peltier cooled incubator (catalogue number 3915FL) at 30°C under a 14 h light and 10 h dark cycle [37]. A 75 W light-emitting diode (LED) Grow Panel (model number HY-MD-D169-S-75W-RB-US) was used inside the incubator to maintain the light and dark cycles. SVM media is prepped following a previously tested recipe by the Olson Lab (2017). AlgaGro® medium is purchased in 50× concentrate from Carolina (catalogue number 153758) and diluted in Poland Spring water per instructions from the manufacturer. Every time new *Volvox* are used for experiments, the entire culture flask is gently mixed and placed in front of a light source for at least 5 min to allow active *Volvox* to move to one side of the flask for easy collection of 1–2 ml of between 500 and 2000 viable *Volvox* colonies.

2.2. Light-stimulation apparatus and imaging

Initial experiments with *V. aureus* were done in ABS plastic chambers printed by a fused deposition modelling (FDM) three-dimensional printer, with clear polystyrene plastic glued to the sides for light access.

Light stimulation was achieved using standard through hole blue LEDs (from Mouser Electronics, catalogue number 630-HLMP-CB1A-XY0DD) with a wavelength of 470 nm and an opening angle of 15°, controlled with an LED driver from Thorlabs (part number: LEDD1B), dialled to power output 1 mm from the LED of 2 mW. To calibrate the LEDs to equal outputs, LEDs were pre-sorted to similar outputs and then soldered into a parallel circuit with a potentiometer in series with every individual LED. Then, light intensity was measured using a photometer probe from Thorlabs (part number: PM130D) at two distances, right at the LED and at 6 cm away from it, after which the angle of the LED and the resistance of the potentiometer were adjusted to achieve a good match of intensities from row to row, as well as from side to side.

Quantification in this set-up was achieved through a collection of *V*. aureus colonies in the different sections with subsequent manual counting using still images of the collected colony ensembles. Plots of phototactic biases using the set-up shown in figure 1 only consider the approximate position of *V. aureus* in the end sections of the chambers that show a more pronounced bias due to the length of the chamber when compared with the second set-up shown in figure 2, which allows for less swimming back and forth.

All light experiments performed on *V. carteri* used SK9822 individually addressable RGB LEDs. with total light outputs above the LED at 2 mW each. Light patterns were programmed using Arduino Nano Controllers (code available at https://github.com/Fw-Franz/Volvox). Housings for adaptive cultures were printed with ventilation holes reaching from underneath upwards between LEDs and culture flasks to aid in heat distribution. Phototactic experiments were performed with only the blue light from the LED at 460 nm, while growth experiments and oxygen measurements were performed at both blue and red (650 nm) light to match incubator conditions.

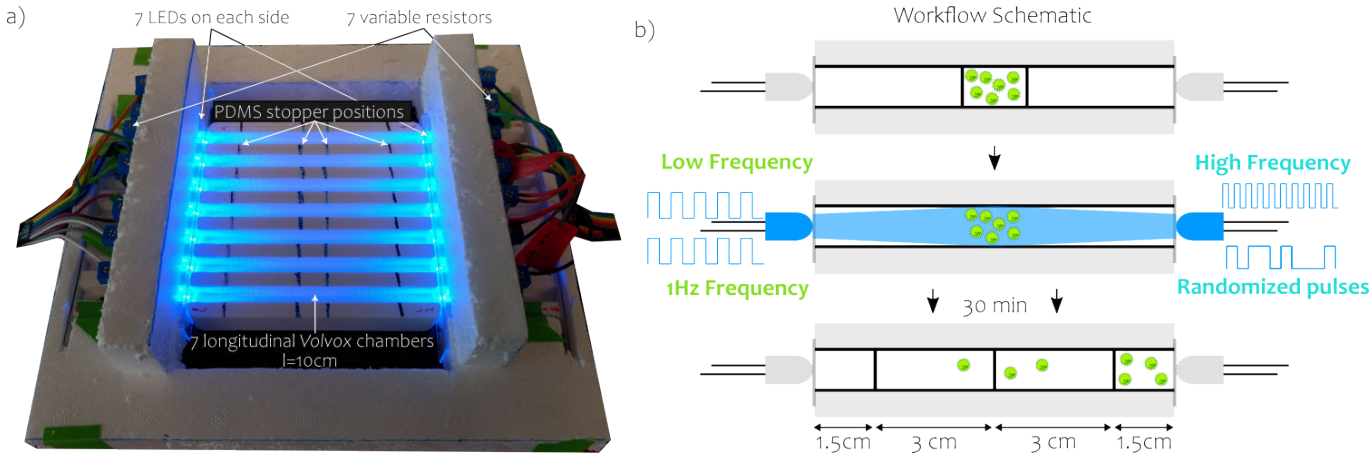

Figure 1. Apparatus and workflow for manual counting of phototactic biases. (a) Phototaxis set-up. Blue LEDs (470 nm) mounted to the side of 10 cm long chambers illuminated the inside of the chamber with blue light. (b) Experimental schematic. An average of 20–30 *V. aureus* were inserted into the middle of each medium-filled chamber ('lane') using a pipette. The middle section of each lane was delimited from the rest of that lane by clear, watertight cast polydimethylsiloxane (PDMS) stoppers of 6.6 mm diameter. Once all the *V. aureus* were added, stoppers were removed from all lanes, and the light pulse series was started on both sides simultaneously. After 30 min, the program ended, at which point stoppers were inserted at the middle and endpoints, and the medium with *V. aureus* was removed from each section and *V. aureus* were counted under a microscope.

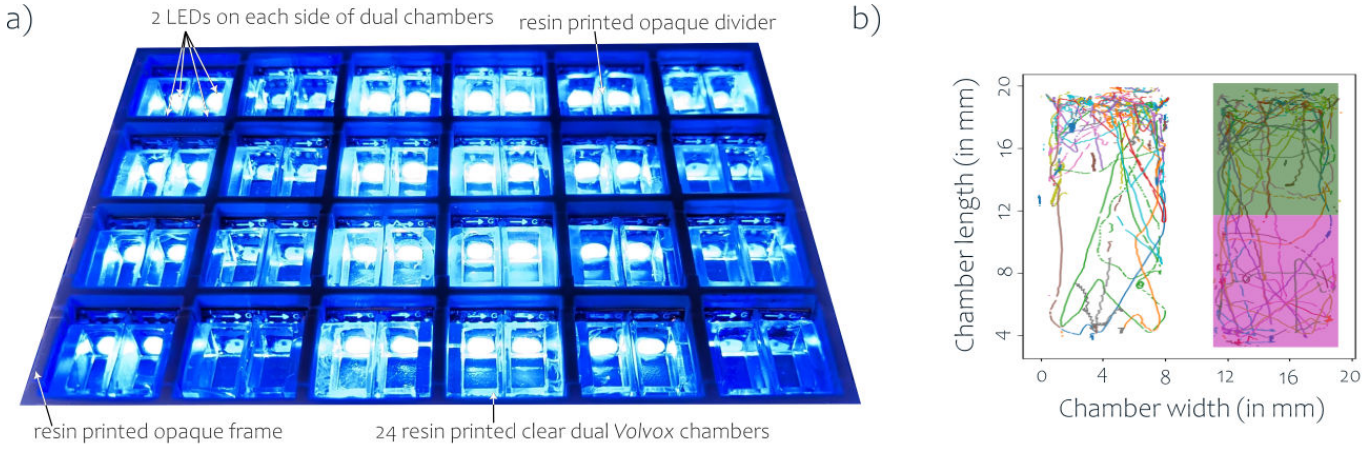

Figure 2. Apparatus and workflow for automatic tracking of phototactic biases. (a) Individually controllable blue LEDs in 48 chambers were pulsed in different lights. (b) Quantification of *V. carteri* phototactic bias was performed based on computational tracking of the images acquired with the MCAM camera array above the chamber. The different colours of the tracks indicate the swimming trajectories of individual *V. carteri* colonies, while the shaded areas in green and magenta on the right indicate the two halves of the chambers closer to either of the two opposing light sources, such as a fixed 1 Hz light pulse frequency, colour coded throughout this article in green, versus a randomized light pulse sequence, colour coded throughout this article in magenta.

Using the MCAM Gigapixel Multi-Camera array of 24 cameras, up to 48 individual chambers (two per camera) can be observed at high spatio-temporal resolution simultaneously with individual light pattern stimulation for each chamber.

Three-dimensional printed clear dual chambers with an optically opaque divider inserted between the two chamber halves to reduce light contamination from the sides are inserted into the device for experiments with *V. carteri* and are removable. Autofluorescence of *V. carteri* was detected at a peak wavelength of 695 nm using a near IR long pass filter with a pass-through wavelength of 685 nm, where the excitation light was the blue light from the LED light at 460 nm. Prior to phototactic experiments in the MCAM camera array, *V. carteri* were dark adapted for at least 2 min.

2.3. Computational tracking and analysis

To analyse the movement of *V. carteri*, a Python (v. 3.10) program was created that utilizes the trackpy library (version 0.4.2, https://soft-matter.github.io/trackpy/v0.4.2/) to track the particle trajectories. The program takes in multiple parameters including, but not limited to, the following: size, speed and integrated light intensity of each *V. carteri* colony, x and y midpoints of the chamber and the number of *V. carteri* colonies. Additionally, the program can adjust for *V. carteri* that are stationary during most of the tracking, so that they can be counted separately for further analysis or excluded in the counting analysis to remove *V. carteri* that are stuck to a surface due to their flagella getting caught to imperfections on the chamber surface. As these imperfections have been reduced heavily by sanding and clear coating of the chambers, this only applies to a small proportion of *V. carteri* and no bias towards different light patterns was observed, as the mechanism is unrelated to the light. The program then takes the filtered information and determines the precise position within each chamber of each *V. carteri* colony

in each time frame. As photo biases did not change drastically over time, we used the average position over the duration of the experiment for statistics and plotting.

2.4. Simulations of cellular photoadaptation in *V. carteri*

Simulations of cellular photoadaption in *V. carteri* in response to different light patterns employ the empirically determined model developed by Drescher *et al*. [18]. While we refer to their work for more detail on the model, we proceed to provide a short summary of our implementation of their model.

The model by Drescher *et al*. is centred around a system of coupled differential equations governing the photoresponse of individual flagella pairs on the surface of *V. carteri* colony spheres, which are of the form

$$\frac{dp}{dt} = \frac{(s-h)H(s-h)-p}{\tau_r},$$
$$\frac{dh}{dt} = \frac{(s-h)}{\tau_a}, \tag{2.1}$$

where $s(t)$ is the dimensionless light stimulus with $s \in [0,1]$, $p(t)$ is the photoresponse variable that correlates with light activation, $h(t)$ is a photoadaptation variable representing the hidden biochemistry, H is the Heaviside step function that ensures a reduction in light cannot increase flagellar beating above base levels and finally τ_a and τ_r are the adaptive and response time constants governing the temporal aspects of photoadaptation.

From this, the measurable fluid speed u generated by the flagella pairs just above the surface of the colony is calculated by solving the pair of differential equations above using the function *solve_ivp* from Python package *scipy.integrate*, with

$$u = u_0(1-\beta p), \tag{2.2}$$

where u_0 is the base fluid speed (experimentally determined by Drescher *et al*. at 81 $\mu m\, s^{-1}$) and $\beta > 0$ quantifies the amplitude of decrease in fluid speed in response to light, which varies across the colony surface, but is set to 1 in our calculations for simplicity without loss of generality.

2.5. Electric shock treatment

2.5.1. Chamber configuration

A three-dimensional printed 30 × 20 × 2 mm chamber as shown in figure 3 was resin printed. A platinum iridium wire (catalogue number AA10056BS) electrodes of 0.5 mm (diameter) were inserted through holes printed on either side of the chamber allowing 1 mm of the electrode to be exposed within the active area of the chamber. An additional chamber stage was printed to act as a holder for a strip of LED lights. The lights were controlled through an Arduino microcontroller, with programs determining the intensity of light.

2.5.2. Voltage and current control

Current was delivered using an LED driver (part number LEDD1B), the current limit was set at 0.2 A and dialled until the voltage in the chamber was measured at the desired level of 3 V, then balanced with resistors in parallel to lower the actual current going through the chamber to non-destructive levels. Measurements were done using a multimeter. An Arduino Nano microcontroller was used to modulate the current. Fixed pulse current was delivered at 1 Hz frequency, and the same random pulse pattern was used for the random light pulse sequences.

2.6. Long-term light pattern treatments and oxygen measurements

Long-term light pattern exposure of *V. carteri* was achieved in dome-shaped three-dimensional printed devices with inbuilt LEDs and ventilation holes on the bottom, and open space towards the top of the culture flask, but shielding the culture flasks from the rest of the incubator lights during treatment. For the long-term experiments, a *V. carteri* culture was expanded into four cultures, one of which was kept under normal incubator conditions, while the remaining three were inserted into the aforementioned dome device under the same fixed 1 Hz, random and continuous light patterns as used in the phototactic experiments. Overall LED output was set to the same level as the incubator lights using the photometer from above. These *V. carteri* cultures alone were grown in the AlgaGro® for increased stability.

For measurements of oxygen production of *V. carteri* in response to light, we used the Firesting o2® apparatus from pyrotechnics, which measures oxygen concentration in a vial in gaseous or aqueous form by scanning an oxygen-sensitive sensor spot inside the glass vial from the outside with an optical fibre probe. *Volvox carteri* cultures were expanded 2 days

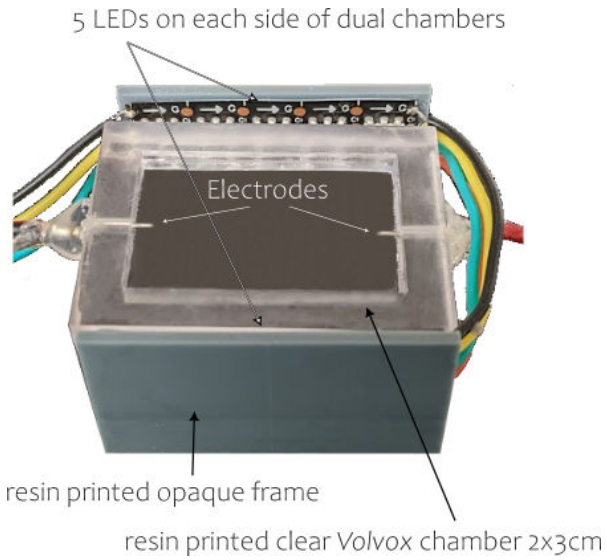

Figure 3. Pulsed electric shock apparatus with adaptive phototaxis. A 30 × 20 × 2 mm chamber with platinum electrodes for stimulation of *V. carteri* through electric current was embedded in an opaque frame with 5 LEDs on each si for dynamic light stimulation during trials to test the ffect of patterened electric shock stimulation on adaptive phototaxis.

before the start of treatment into four flasks of 200 ml each, then, before the start of treatment, combined in a conical tube, gently inverted to thoroughly mix the cultures and then separated into four new flasks. One was left as control in the incubator, while the other three were exposed to light in the dome-shaped three-dimensional printed devices described above. Oxygen measurements were taken before treatment, and then after 6, 24, 30 and 48 h, respectively, by slowly and gently swirling each flask to mix the media but not to agitate and add more oxygen, then gently and extremely slowly transferring 5 ml using a Pasteur pipette of one culture into the oxygen measurement vial with a temperature probe in it for temperature compensation of oxygen concentration measurement.

3. Results

3.1. *Volvox* distinguish between patterned and random light stimuli

To investigate the ability of *Volvox*, starting with *V. aureus*, to detect and differentially react to temporal light patterns, we designed three-dimensional printed chambers of different sizes, consisting of isolated channels with clear ends, each end illuminated by a separately microcontrolled LED, with manual counting (figure 1) and camera-based tracking (figure 2). Based on our central hypothesis of surprise minimization in aneural organisms, we tested the prediction that a phototactic organism such as *V. aureus* would reveal a preference for order (or a dislike of unpredictability) by preferentially moving towards light stimulation patterns of higher regularity (and hence predictability). When we exposed *V. aureus* to an overall equal amount of light over time but at a regular, fixed light pulse interval versus a randomized, irregular light pattern (see figure 4), a significantly larger proportion of *V. aureus* were detected in the section adjacent to the fixed interval stimulation than in the section adjacent to the random stimulation ($p < 0.05$, Wilcoxon signed-rank test), in accordance with our predictions based on uncertainty minimization.

Because of this observed preferential movement of *V. aureus* to the regular 1 Hz light pattern when opposed with a randomized light pulse pattern of similar average pulse length, we conclude that *V. aureus* can distinguish patterned light stimuli from random ones, a fundamental building block for intelligent information processing [38,39].

To minimize sources of error and bias from manually counting *Volvox* and to get real-time data on *Volvox* photoadaptation for downstream data mining, we also designed and tested a system that combines highly transparent smaller chambers (reducing the effect of light scattering) with a high-resolution camera system. For this system, we chose exclusively *V. carteri*, as we have a more detailed understanding of its photoadaptive mechanism on which we can rely to interpret the tracking data gained from our experiments using this set-up. We used this apparatus to test the same hypothesis on another species of *Volvox*, *V. carteri*, which is evolutionarily distant from *V. aureus* by an estimated 75 Myr [40].

Our results in this automated platform show that, as for *V. aureus*, *V. carteri* also exhibits a photoadaptive bias towards a regular light pulse pattern versus a random one (see figure 4*a*), as over time, more *V. carteri* swam closer to the patterned stimulus side than to the randomized stimulus side ($p < 0.01$). From this, we conclude that despite the physiological difference between both species, the phototactic biased behaviour predicted by uncertainty minimization was present in both species, which constitutes strong evidence for uncertainty minimization as ubiquitous behavioural directive in aneural organisms.

We exploited the detailed quantitative nature of this imaging apparatus to investigate the influence of *V. carteri* colony size (µm), swimming speed (µm s^{-1}), and the number of colonies inside the chamber on its phototactic bias using a principal component analysis (PCA), where the range of these variables was 138–171 µm, 71–670 µm s^{-1} and 8–38 respectively, rounded to the nearest integer. A graphical representation of the distribution of those three variables can be found in electronic

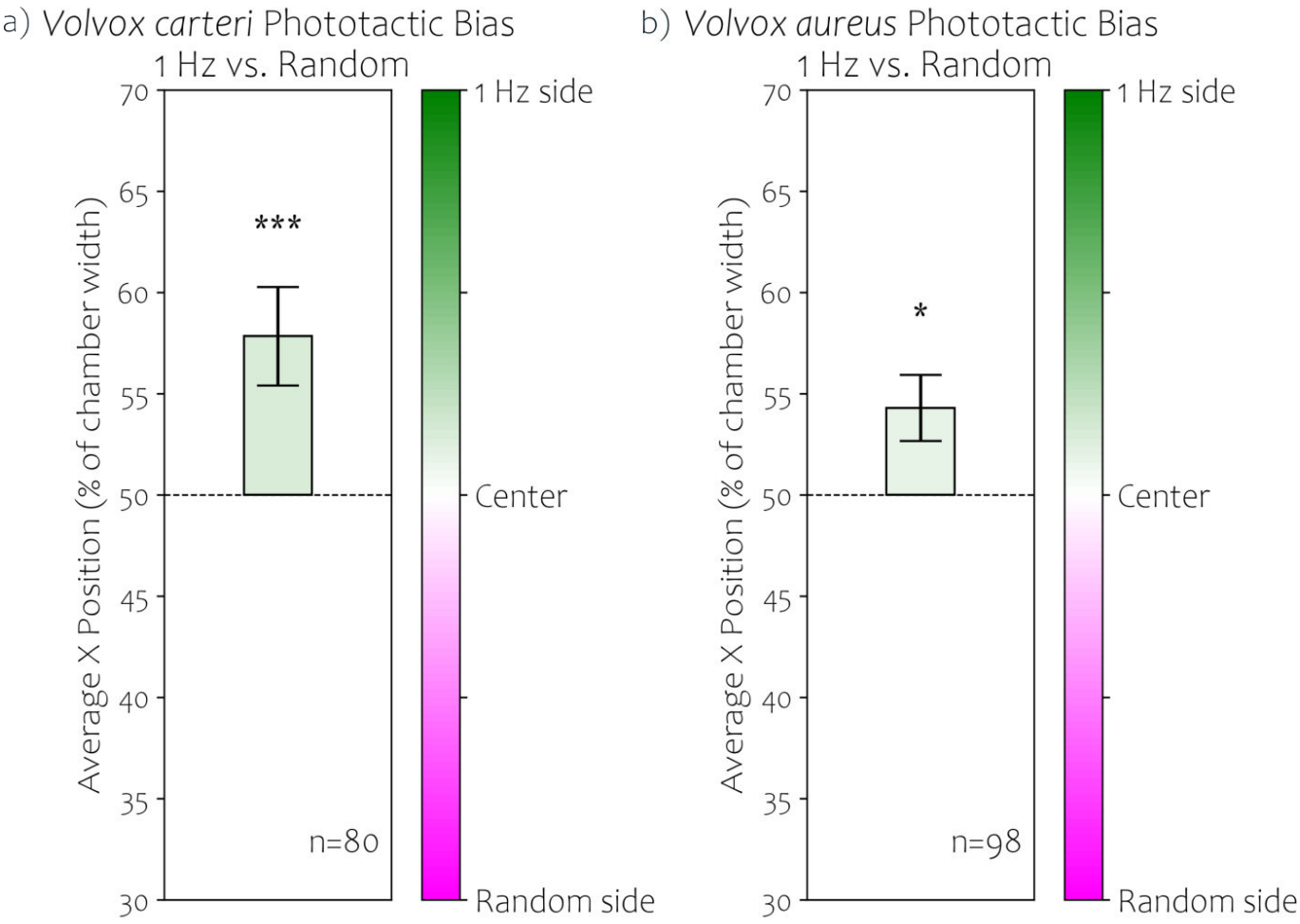

Figure 4. Photoadaptation in *V. carteri and aureus* exhibits a bias against randomized light pulses. *Volvox carteri* and *V. aureus* prefer fixed (1 Hz, 0.5 s light duration) over random light pulse series. (a) *Volvox carteri* phototactic bias was quantified as indicated in figure 2. Plotted is the average *x* (along the major axis of the chamber) position in per cent relative to the chamber width for each experiment (*** indicates $p < 0.001$, Wilcoxon signed-rank test). (b) Phototactic preference in *V. aureus* was measured by counting *V. aureus* colonies that were collected in one end of the well versus the other (see figure 1), after which the average *x* position was approximated in the same manner as in (a). A significantly larger proportion of *V. aureus* was detected in the section closer to the fixed interval stimulus than the randomized stimulus (* indicates $p < 0.05$, Wilcoxon signed-rank test).

supplementary material, figure S1. The PCA revealed that the first two principal components accounted for 91.07% of the total variance in the data, with PC1 explaining 56.72% and PC2 explaining 34.35%. The third component, PC3, accounted for the remaining 8.94% of the variance. The component loadings for each variable are presented in table 1.

The strong positive loading for both *V. carteri* colony size and swimming speed in PC1 suggests a robust positive correlation between these two variables, indicating that larger *V. carteri* colonies tend to swim at higher speeds in our system. This relationship could be attributed to the increased propulsive force generated by larger colonies with more flagellated cells.

The strong negative loading for the number of colonies per frame in PC2 suggests that this component appears to represent colony density, largely independent of size and speed. The moderate negative loading for speed on this component suggests a slight tendency for lower swimming speeds in frames with higher colony counts, possibly due to increased hydrodynamic or direct flagellar interactions, leading to *V. carteri* colonies getting stuck to each other temporarily. PC3, while only explaining 8.94% of the variance, revealed an interesting contrast between colony size and swimming speed. This minor component might capture exceptions to the main trend, possibly representing scenarios where larger colonies move more slowly or smaller colonies move more quickly and could be related to variations in colony morphology, flagellar activity or local environmental conditions.

The high cumulative variance explained by PC1 and PC2 (91.07%) indicates that the three-dimensional data can be effectively represented in two dimensions with minimal loss of information. This suggests a strong underlying structure in the *V. carteri* population dynamics, primarily driven by the size–speed relationship and variations in colony density.

Based on this analysis, we filtered *V. carteri* by size (colony diameter between 120 and 150 µm) and swimming speeds (larger than 120 µm s^{-1}) in the analysis of the trajectories for higher uniformity and standardization of our data. Thus, the most effective distinction between the random and patterned stimuli was being carried out by *V. carteri* of that size and swimming speed.

Table 1. PCA component loadings. PC1, explaining the majority of the variance (56.72%), showed strong positive loadings for both *V. carteri* colony size and swimming speed. PC2, accounting for 34.35% of the variance, was predominantly characterized by a strong negative loading for the number of colonies per frame.

variable	PC1	PC2	PC3
colony size	0.941450	0.064707	0.365889
swimming speed	0.900969	−0.298521	−0.351469
number of colonies	−0.212085	−0.980930	0.131096

3.2. *Volvox* show optimal photoadaptation to specific frequencies

We next examined which light pulse frequencies, if any, *Volvox* most readily adapt to—by exposing *Volvox* inside the channel to different light pulse frequencies on each side of the chamber. Using first the manual tracking set-up with *V. aureus*, we tested various pulse frequencies from 50 to 1 Hz and determined the per cent of *V. aureus* that swam to each end of the chamber (see figure 5). There was a clear preferential adaptive response to light pulse frequencies of 2 Hz when opposed to smaller and larger pulse frequencies, respectively ($p < 0.001$ as determined by Wilcoxon signed-rank test). From this, we conclude that *V. aureus* distinguish different regular patterns in terms of their adaptive, phototactic response.

Using the automated tracking apparatus, we also tested the presence of phototactic biases in *V. carteri* for the highly significant case of 1 Hz versus 2 Hz in *V*. aureus. However, unlike in *V. aureus* (see figure 5), in *V. carteri* there was no difference between photoadaptive responses to either opposing light stimuli of 1 and 2 Hz, respectively. We only compared two frequencies, so it is very possible that photoadaptation in *V. carteri* is optimized to a different frequency range than in *V. aureus*, possibly due to slightly different flagellar response times, overall rotational speed or resonant tuning of the two compared with *V. aureus*. These differences would need to be investigated in future studies, as no such detailed studies have been done on *V. aureus*. Note that flagellar beating frequencies in *V*. carteri have been previously determined to average at 39.3 Hz [41], much higher than the light pulse stimulation frequencies used in the experiments here, and are hence unlikely to have influenced phototactic biases in our experiments, as they are too fast to interact with the experimental stimulation.

The data from §3.1 on the patterned versus randomized light sequences, combined with these data on different light pulse frequencies in two similarly simple aneural species, support the hypothesis that even aneural organisms can detect patterns and tend to avoid random stimulation patterns precisely because of the difference in overall predictability of those stimulation patterns, and not just due to differences in frequency.

3.3. Simulation using a cellular scale *in silico* model of *V. carteri* response to random versus patterned inputs predicts that uncertain inputs decrease photoadaptation

In order to probe how uncertainty minimization is implemented mechanistically on the level of individual somatic cells that biochemically implement the photoresponse, we built on work by Drescher *et al*. [18], who measured fluid speeds in the vicinity of individual somatic cells in response to light activation as a measure of flagellar beating modulation to construct their photoadaptive model, to simulate the adaptive phototactic response of *V. carteri* to the same types of input used in our experimental system above (figures 1 and 2).

We simulated fluid speed changes caused by flagellum beating speed downregulation in response to inputs reflecting fixed 1 and 2 Hz versus randomized light pulse stimulations with similar average interval lengths and equal total light exposure. The average adaptive, or recovery time (the time it takes for a flagellum to return to baseline beating frequency after photostimulation), obtained for the irregular, randomized light input series was increased (see figure 6e) compared with the fixed pulse sequence (figure 6c). Not only did the average fluid speed return to lower base levels for the random sequence compared with the fixed treatment but there was also a much higher variation around its mean recovery, which is likely to contribute to interfere with overall photoadaptation on the organismal level, as that noise further decouples adaptive time from the colony rotation period.

Given the ubiquity of Poisson-distributed neuronal activation patterns in neural organisms [42], we confirmed that when we randomized inputs by shuffling stimulation pulses (which constrained each stimulation to yield similar average pulse duration and equal total light exposure), the histogram of inter-pulse durations exhibited a Poisson distribution (see figure 6f).

Interestingly, this is the distribution most used to model natural pulsed stimulation patterns in human brains [42] to avoid adaptation through habituation to repeated stimuli. As seen below, this opens up research on short-term adaption in *Volvox* as a foundation for learning, as Poisson-type stimulation patterns have been shown to evoke distinct spike timing-dependent plasticity (STDP) in neurons [43]. In other words, neural systems react very differently to purely random Poisson-distributed spike trains versus tightly regulated, repeatable activation patterns, the balance thereof being an active source for debate and probably varies in different neuronal systems depending on how tightly information is compressed at each level [44,45].

Since the ability of *V. carteri* to maintain directionality in phototaxis is immensely time-constrained by their rotational frequency (which is colony size dependent and falls between 0.5 and 3 rad s^{-1} for colonies between 100 and 200 µm diameter and is closely matched with the photoresponse [18]), we can hypothesize that a Poisson-distributed light stimulation pattern

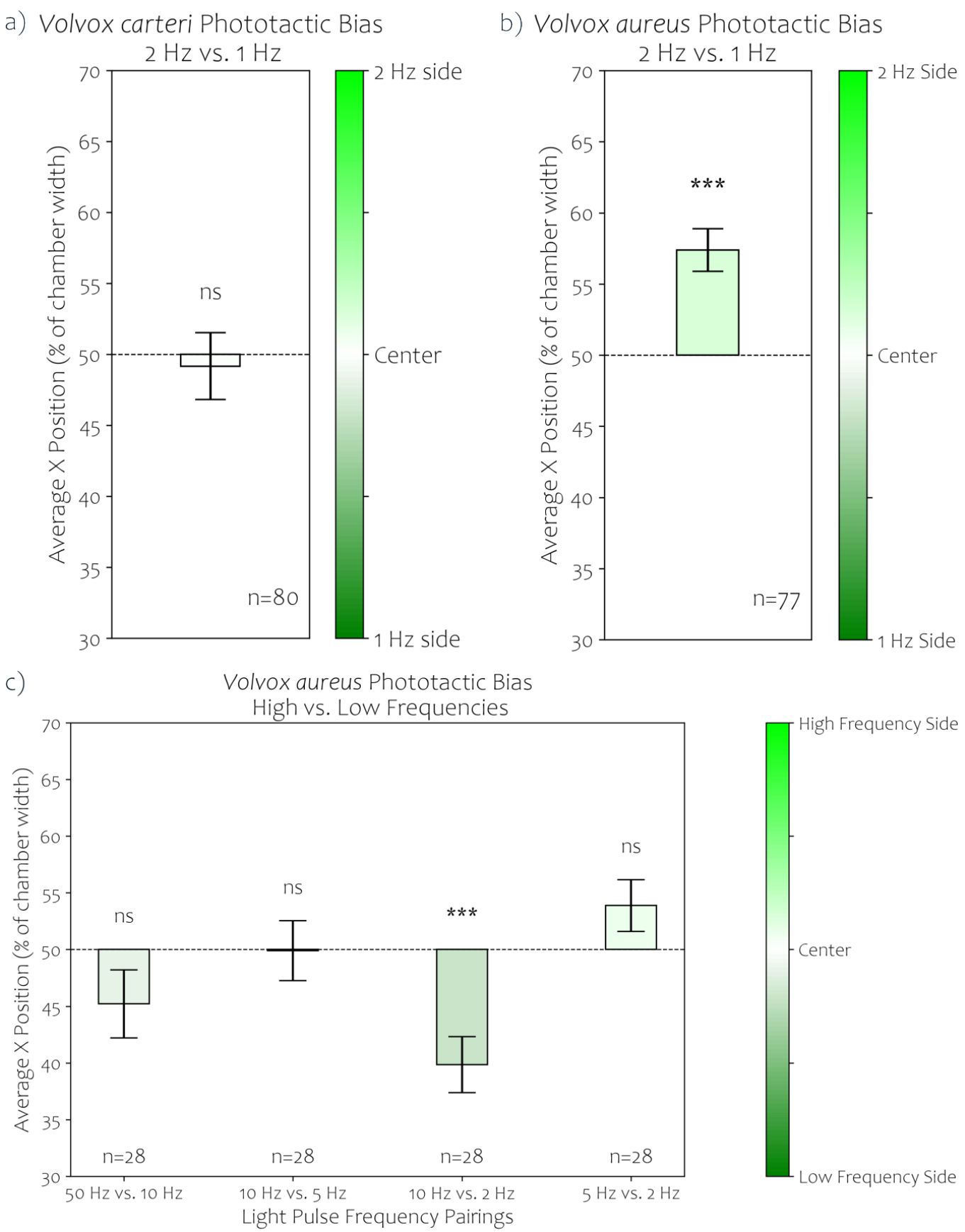

Figure 5. Photoadaptation in *V. aureus* and *V. carteri* is optimized for different specific light frequencies. No significant phototactic bias was observed between 1 and 2Hz stimuli for *V. carteri*. Data were collected using the automatic tracking set-up described in figure 2. For *V. aureus,* however, a very significant (*** indicates $p < 0.001$, Wilcoxon signed-rank test) bias was observed towards the 2 Hz side. This indicates a difference in photoresponse between the two species. (c) Different light pulse frequency pairings reveal a lack of biases in frequencies higher and lower than 1–2 Hz, while a stronger bias towards 2 Hz was observed against 10 Hz, indicating a window of optimal photoadaptation in *V. aureus* towards 2 Hz. Data for (b) and (c) were collected using the manual counting set-up described in figure 1.

will interfere with their ability to maintain their direction. This is because, by decreasing calcium signalling, such randomized activation patterns would effectively decouple colony rotation from photoactivation, whose evolved interdependency is at the

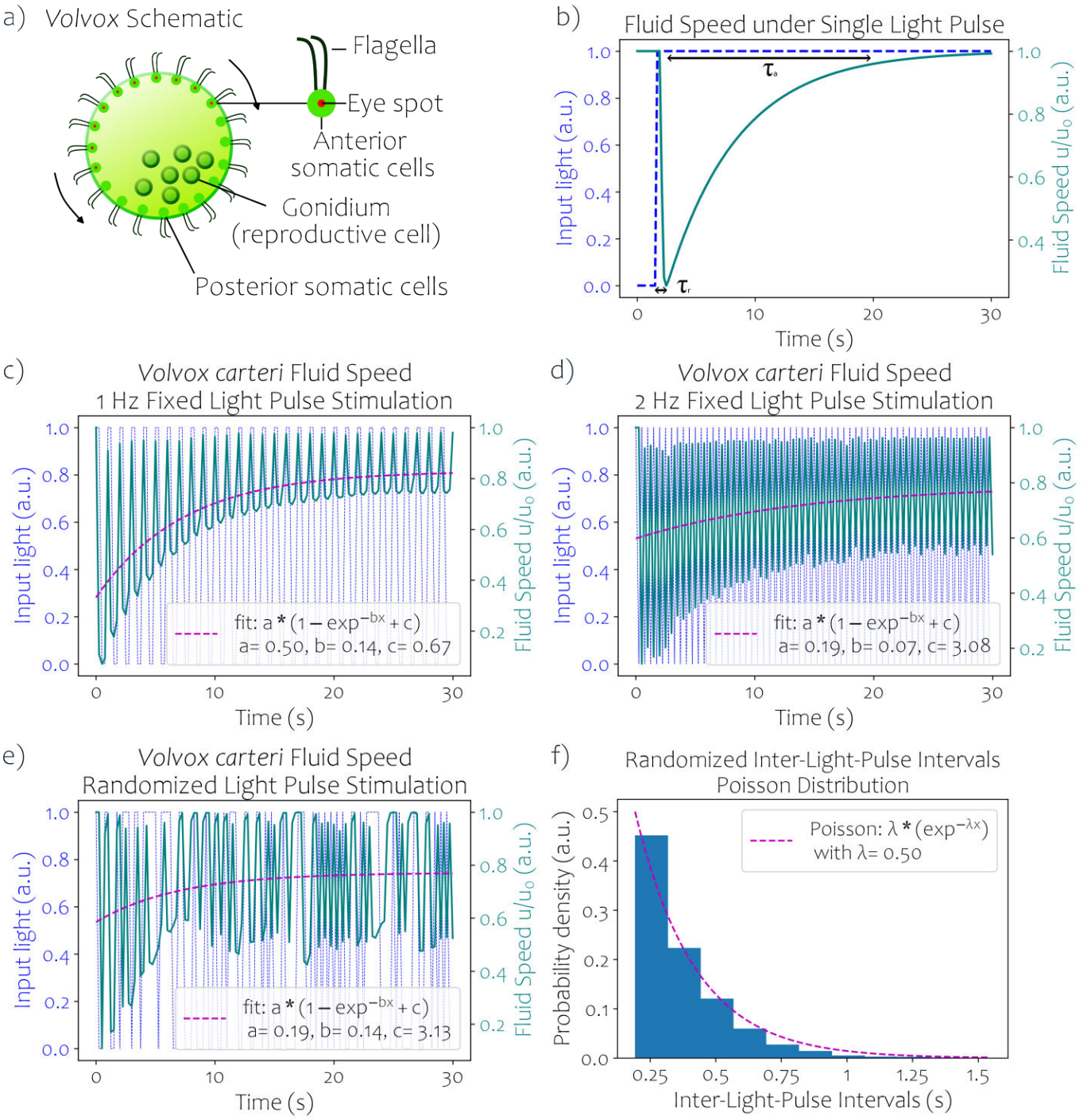

Figure 6. Simulation predicts that randomized inputs decrease adaptive phototactic response in *V. carteri*. *Volvox carteri* organismal colonies exhibit an adaptive response to light by virtue of their eyespots, which when stimulated by light downregulate flagellum beating speeds, resulting in biased movement towards the light. (a) A schematic of *V. carteri*. A *V. carteri* organism (also called colony) consists of typically 5–10 reproductive cells in the interior, and up to 2000 vegetative cells on the exterior, each equipped with two flagella that exert net force around the *V. carteri* colony towards the posterior side, moving it forwards through water. Anterior cells also possess an eyespot that allows light sensing. (b) *In silico* modelling of *V. carteri* photoadaptation (based on the equations from Drescher *et al.* [18]). When a light stimulus is presented to a *V. carteri* colony, eyespots, with higher deactivation strength in the anterior region of the *V. carteri*, downregulate flagellum beating speed within a sub-second time window, which causes the organism to rotate and align its anterior–posterior axis with the direction of the input light. This adaptive downregulation of flagellum beating frequency is transient and recovers after a few seconds. Because of a slight torque in the *V. carteri*, the organism can prevent misalignment by stabilizing this adaptive recovery period, exposing different eyespots to the light as the organism rotates along its own axis. (c–e) As simulation inputs, we used both fixed light pulse intervals with frequencies of 1 Hz (c) and 2 Hz (d), as well as randomized (e) pulse intervals with similar average interval lengths to stimulate flagellar beating downregulation over time. The average adaptive (or recovery) time (the time required for flagellar beating to return to baseline) is much longer for the randomized input, which is also quantified by fitting an exponential decay curve to the patterns. Specifically, variations around the fitted mean of the adaptive rate are increased over twofold for the randomized sequence compared with the fixed pulse sequence, which would heavily interfere with correct colony orientation towards light. (f) A computed histogram of the inter-light pulse intervals for the randomized stimulation sequences shows that they are Poisson distributed.

heart of how *V. carteri* maintain phototactic direction in the first place. Interestingly, this tuning of flagellar adaptation time to rotational frequency has also been demonstrated in *Chlamydomonas* and *Gonium*, related Volvocales genera, demarking it as an important evolutionary conserved feature [46,47].

Note that while we did not model three-dimensional movement of *V. carteri* in these simulations, their relatively slow average upward swimming speed of 274 $\mu m\,s^{-1}$ and max fluid speeds of 400 $\mu m\,s^{-1}$ [41] compared with the ratio of chamber length (2 and 10 cm for the imaging and manual counting set-up, respectively) and light pulse frequencies mean that the effect of colony displacement on light amplitude changes can be considered negligible compared with rotational frequencies.

3.4. Temporal selectivity of *V. carteri* photoadaptation is altered by a calcium channel blocker targeting primarily internal calcium channels

We next investigated the mechanism underlying the temporal preferences we observed in phototactic outcomes both *in silico* and *in vivo*.

First, we characterized how components integral to the modularity of the adaptive photoresponse (i.e. light activation and recovery time of downregulated flagellar beating speed) are implemented in *V. carteri*. While initial calcium currents upon light activation peak between 1 and 25 ms depending on the stimulation light intensity in this organism [48], far outside the regime of rotational time periods (approx. 2–12 s) and flagellar beating modulation (approx. 50–400 ms), its diffusion across the flagella has been estimated to take an average of 200 ms [18], which is in the same order of magnitude as flagellar beating modulation, with response times τ_r around 200 ms for normal light intensities [18]. We used nimodipine, a reagent commonly used to selectively inhibit calcium signalling [49,50], which was previously shown in the close *V. carteri* relative *Chlamydomonas*, to bind to a calcium inhibitor binding protein localized primarily in the cell-internal membrane [51].

This enabled us to observe the adaptive response of *V. carteri* to light inputs in real time during the inhibition of signalling from the photoreceptor to the flagella (figure 7). As blocking calcium this way slows down the calcium-mediated signal progression from photoreceptor towards flagella, thereby causing a decrease in phototactic sensitivity [51], we can describe this effect in *V. carteri* as an increase in the photoresponse time τ_r introduced earlier.

Note that we shifted the speed filtering criteria for nimodipine containing media for lower speeds, as nimodipine also reduced overall maximum speeds as a consequence of lowered phototactic sensitivity (see electronic supplementary material, figure S2).

We tested whether such a decrease in internal calcium flow rates causes a shift in the frequency dependence of phototactic preference. We found that in the presence of nimodipine, *V. carteri* showed a significant phototactic bias towards the 2 Hz stimulus compared with the 1 Hz, while preference for the 1 Hz regular stimulus compared with the random pulse sequence reversed. Based on these results and the known mechanism of action of nimodipine as a calcium channel blocker interfering with internal calcium flow in Volvocales, we have hence shown that calcium signalling is required for maintaining the temporal fidelity of photoadaptation and that inhibiting it partially decouples the photo-induced, calcium-mediated flagellar modulation from colony rotation as phototactic biases towards set frequencies or patterns were shifted in our experiments.

To further elucidate this phenomenon, we turned back to the simulations from §3.3 and simulated the fluid speed induced by flagellar beating in response to the same 2 Hz frequency as before under the effect of nimodipine. Nimodipine, through its mode as a calcium channel blocker, reduces calcium flow into the flagella and hence the speed of information flow from photoreceptor to flagellar that determines its photoresponse time, so we increased the response time in the simulation of photoadaptation τ_r by a somewhat arbitrary factor of 5. Its exact value would need experimental validation through high-speed imaging of flagellar activity and fluid flow in response to the drug at different doses, but the choice was motivated by calcium uptake being accelerated fivefold in normal light activation in Chlamydomonas [51]. While this means our simulations here cannot confirm the exact behaviour of the dose of nimodipine employed, we believe it illustrated the general mode of action in our model at this chosen translated drug dose. We found that while the overall exponential fit was not too different from figure 6e, the decreased response time reduces the overall amplitude of variation over the mean fluid response, making it more similar in shape to the regular step function. This corresponds to shifting the high-frequency light above a flicker fusion frequency (the rate at which photoreceptor responses no longer discriminate between intermittent light pulses) in *V. carteri* photodetection. While the response time was still reduced overall, the reduction in variations may mean there are fewer downstream influences that interfere with normal *V. carteri* phototaxis. This suggests that inhibition of calcium uptake and diffusion shifts the sensed base frequency of the interval lengths that *V. carteri* can perceive, akin to a flicker fusion rate in human vision (and that of less complex organisms such as insects [52]), denoting a maximal light flickering frequency the photoreceptors and downstream processing in vision can no longer perceive as individual pulses.

3.5. *Volvox aureus* exhibit memory persistence towards past light direction

A necessary condition for pattern recognition and tracking over time is the persistence of a stimulus' effect on its internal state over a limited amount of time—a type of memory. To prove the existence of such a persistence of effect in *V. aureus*, we designed an experiment to test if phototactic alignment of *V. aureus* towards one stimulus persists after that stimulus ends. We used

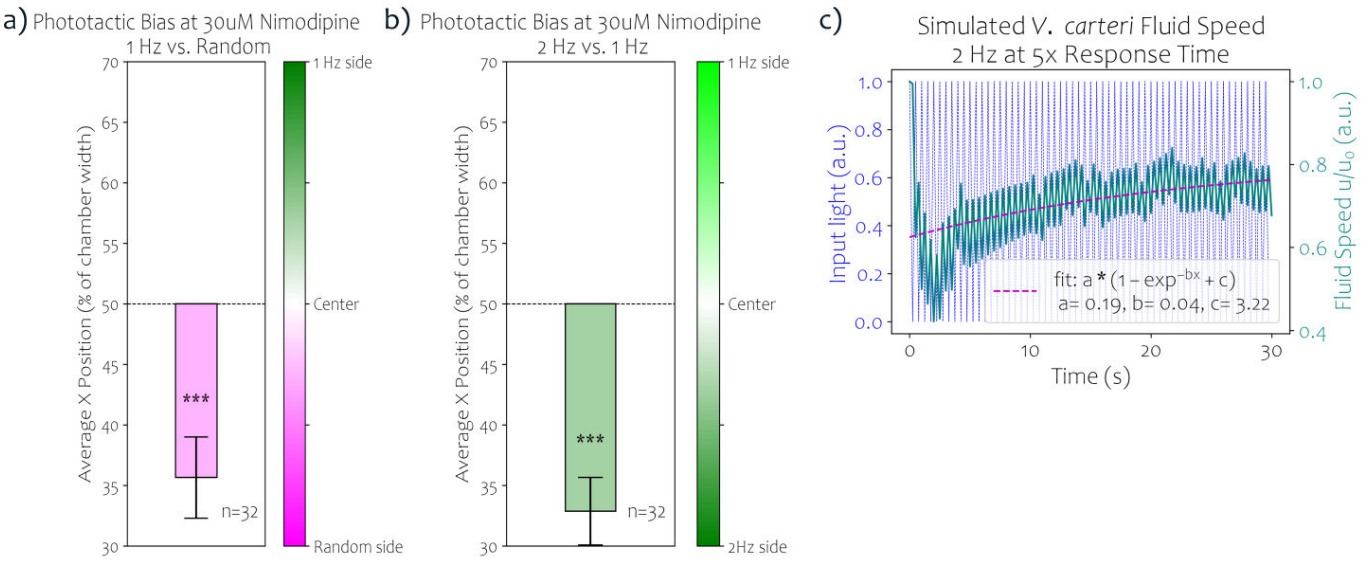

Figure 7. Calcium flow inhibitor nimodipine reverses 1 Hz to random bias and induces 2 to 1 Hz bias. Recording phototactic biases in *V. carteri* in the presence of 30 µM nimodipine revealed significant changes to phototactic biases. (a) A very significant ($p < 0.001$, Wilcoxon rank test) bias was observed towards the random light side for nimodipine treated *V. carteri*. (b) Inhibition of calcium release and downstream diffusion along the flagella caused by nimodipine shifts phototactic preference to higher frequencies of 2 Hz, which was lacking in the *V. carteri* without the drug. (c) Simulations of increased response time τ_r hypothesized to be caused by nimodipine show drastically lowered variations around the mean recovery rate plotted by the exponential decay fit normally induced by the high frequency rate as observed in figure 6e.

the experimental platform described in figure 1b and confined *V. aureus* into a 1 cm space at the centre of the channel using transparent dividers and then illuminated them from one side with blue LED light for 5 min.

After this period of illumination in confinement, we turned the light source off and allowed the *V. aureus* colonies to travel freely for 10 min, collecting the *V. aureus* at each section in the well as before. There was a significant ($p < 0.05$, Wilcoxon signed-rank test) bias towards the previously illuminated side of the well, indicating the persistence of phototactic alignment (figure 8).

A likely mechanism of this persistence of effect is a sufficient combination of the initial orientation of the *V. aureus* colony towards light stimulus and the maintenance of that orientation over short time scales even in the presence of small-scale perturbations. It is already known that the first part of that combination occurs: *V. aureus* orient themselves towards light by virtue of the asymmetric distribution of photoreceptor activity along their sphere and flagellar orientation, as is the case for *V. carteri* [18].

The fact that in our experiment, *V. aureus* colonies were still preferentially distributed towards the light stimulus 10 min after it ends is evidence for the swimming orientation in *V. aureus* being stabilized when a light stimulus is removed, which is why our result is the first evidence of short-term memory in *V. aureus*. Note that while the average position of *V. aureus* in the no light control group clustered around the middle of the chamber as expected in the absence of any photostimulation, a total average of 29.2% was found at the end segments at the end of the experiment, indicating that these control colonies were still able to swim freely (but directionless) in the absence of stimulation, as is known of *Volvox*.

3.6. Photosynthesis efficiency is not significantly affected by randomized light pulses compared with the fixed frequency light stimulation pattern

Next, we wanted to find out whether *Volvox* photosynthesis was also affected by different light patterns, especially unpredictable ones, to test the hypothesis that the mechanism by which *Volvox* detect patterns versus randomness involved monitoring of energy generation, and also whether such patterned or random light stimulation would interfere with normal *Volvox* growth.

We quantified photosynthetic efficiency using the Firesting™ (Pyrotechnics) to measure oxygen concentrations, using an external optical fibre probe to scan an oxygen-sensitive sensor inside glass vials containing *V. carteri*. The duration of these experiments was necessarily performed on a different time scale than our phototactic experiments, as the effect of light on photosynthesis takes much longer to result in increases in oxygen concentration in the culture media that the Firesting™ can detect, as opposed to the immediately measurable effect of light on phototaxis. Because the individual sensors are highly sensitive to temperature and media conditions and are not stable in normal *Volvox* culturing conditions over longer times, we were limited to taking measurements at individual timepoints and used a temperature probe inside the vial for temperature compensation. Measuring oxygen concentrations at two timepoints per day, one in the morning and one in the evening, we observed that oxygen levels in the media rose significantly in the continuous light treatment (our positive control) but not in either the randomized light pulse group or the fixed light pulse series treatment (our negative control) (see figure 9).

Because in both experimental conditions, the light was off for 50% of the exposure due to the duty cycle of the light pulse patterns (while both experimental and control conditions experience the normal 14/10 hour day/night cycle necessary for

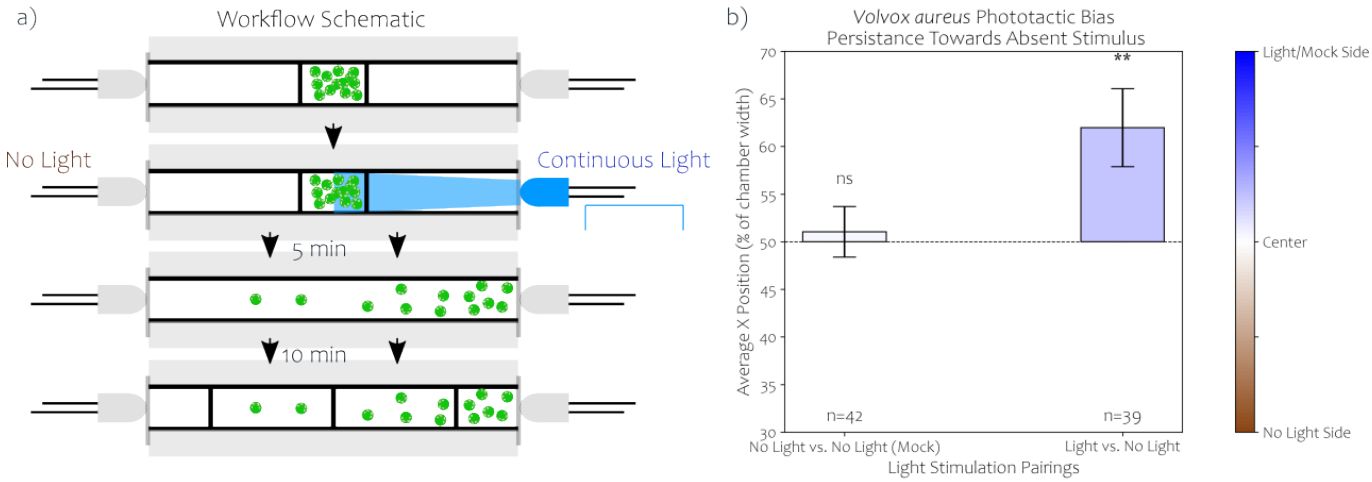

Figure 8. *Volvox aureus* phototactic movement persists for minutes after the light stimulus ends. (a) Workflow schematic. *Volvox aureus* were confined into a space of 1 cm using transparent dividers and then illuminated from one side with blue LED light for 5 min, after which we turned the light source off and allowed the *V. aureus* colonies to travel freely for 10 min, collecting the *V. aureus* at each section in the well as before. (b) A significant bias towards the previously illuminated side of the well was detected 10 min after the light stimulus ended ($p < 0.05$, Wilcoxon signed-rank test), indicating a persistence of phototactic alignment.

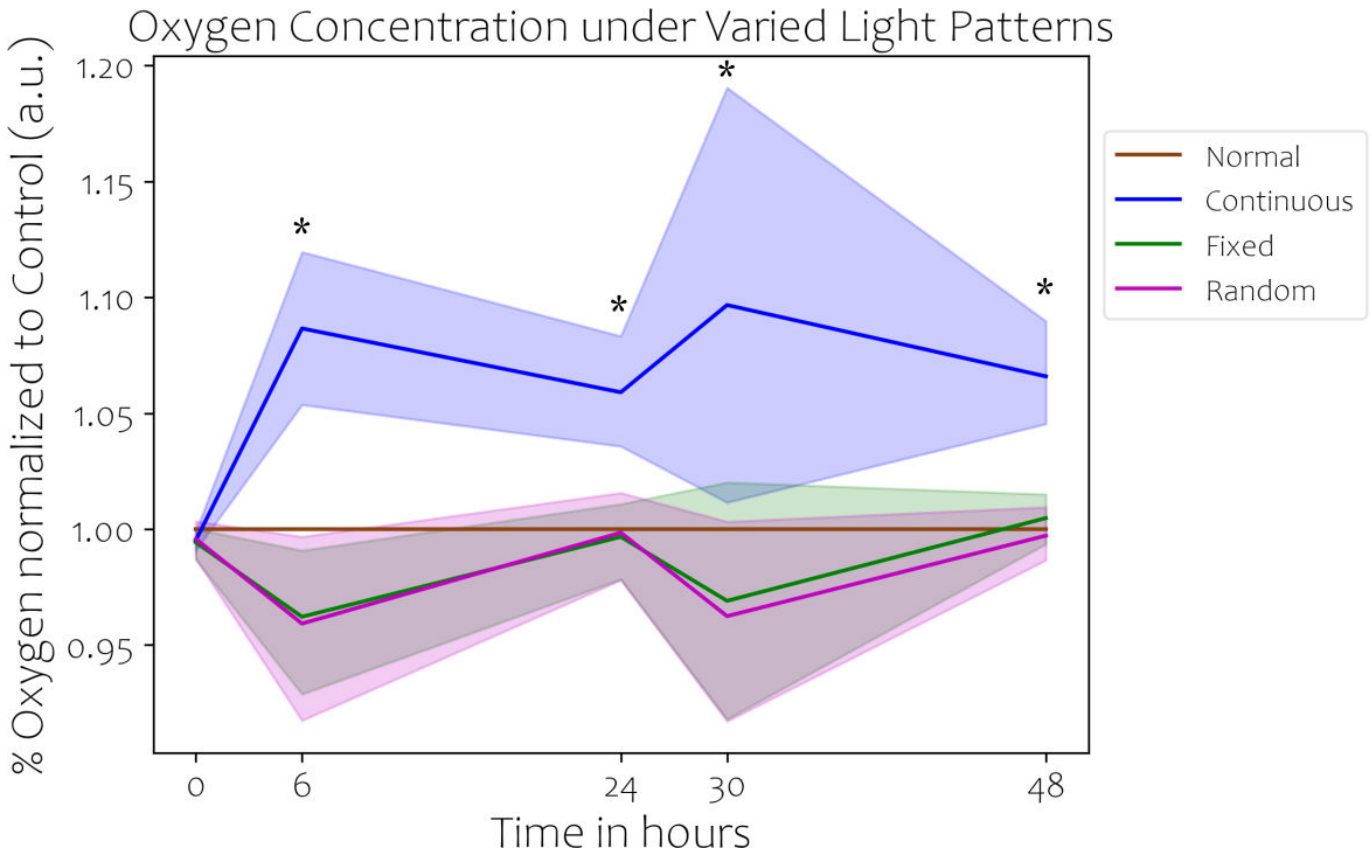

Figure 9. Regular and randomized pulsed light does not increase oxygen concentrations in *V. carteri* media. Line plots of per cent oxygen concentrations over time for each group normalized to that of a control group from the same culture stock maintained in normal incubator conditions, where the 'normal' group refers to *V. carteri* cultured under standard growth lights used for all *Volvox* cultures, as opposed to the LED dome devices described in §2.6, in which the treatment groups were cultured. As expected, the positive control—continuous light treatment (slightly higher light density exposure than provided by the normal incubator lights)—significantly increased oxygen concentration in the medium.

normal *V. carteri* growth), we expected a significant decrease in photosynthesis, which was, however, not detectable with the statistical power of our experiment.

With respect to the longer time scales made necessary by the experimental constraints, the lack of a significant difference in oxygen production between the fixed and random light pulse conditions suggests that random pattern avoidance in *V. carteri* did not evolve simply to maximize energy, but is instead a core feature of the way they process their environment.

3.7. *Volvox carteri* adapt to long-term exposure to patterned culture light

We next wanted to investigate the ability of *Volvox* to adapt in the long term, rather than just in the short term as above, to the same patterned and random light conditions in their culturing environment in time frames close to evolutionary time scales. We asked whether *V. carteri* would adjust their preferences in the long term, by exposing *V. carteri* to the different light conditions for 2 years and then remeasuring their phototactic biases as above.

The result was that *V. carteri* exposed to either light pattern, randomized or 1 Hz light pulse frequency, no longer exhibited a phototactic bias towards the 1 Hz stimulus side (figure 10) compared with control colonies in the same experimental study, which is evidence of pattern-specific habituation in *V. carteri*, which is a form of non-associative learning. This remarkable finding takes the short-term adaptation of the earlier sections on phototactic biases and short-term memory (all in the scale of minutes) to much more long-term changes at the population level in the order of months to years.

While detailed molecular analyses need to be performed on these adapted cultures in future studies to determine how the different cultures adapted on a molecular level, this result is a clear example of a population-level adaptation gained over multiple rounds of cell division based on environmental stimulation patterns in *V. carteri*.

3.8. Patterned electric shocks interfere with photoadaptation

Next, we examined the effect of a different kind of uncertainty-induced stress on photoadaptation. Unpredictable electric shocks have been widely used to increase stress in neural organisms experimentally. A 2016 study of human participants by Berker *et al*. found a high correlation between stress responses, measured through physiological changes including pupil diameter and skin conductance and environmental uncertainty [53]. Linking stress and uncertainty from the external environment could help organisms more quickly adapt to their changing environments providing an advantage both during the organism's lifetime and evolutionarily. However, increased stress as a response to unpredictable environmental stimuli has not been studied much in simpler, aneural organisms, particularly when light and electricity are used as stimuli.

To assess the effect of random electric shocks on photoadaptation, we used a 30 mm chamber in which the light axis and electric current axis were perpendicularly paired. Dynamic lights were used with the light source switching between the top and bottom of the chamber every 60 s. The top lights were engaged for 60 s and then completely turned off while the bottom lights were on for 60 s (see figure 11).

The switching lights provided more opportunities to observe phototactic behaviour and ensured that *V. carteri* would not be directed towards and get stuck at one side. To ensure that there was no physical bias, the stage holding the chamber was levelled and the light intensity of each LED was measured and adjusted to achieve equal brightness output for the top and bottom lights.

When current was applied to the chamber in a continuous fashion, *V. carteri* colonies exhibited consistent phototactic behaviour over the course of the whole 10 min. The *V. carteri* colonies started moving towards the light source strongly as seen by the increase in *V. carteri* in the top quartile.

As the light source location changed, the *V. carteri* then moved more towards the bottom, as seen by the decrease in *V. carteri* in the top quartile and an increase in the number of *V. carteri* in the bottom quartile. While the number of *V. carteri* in the top of the chamber peaked at 100 s and then declined slightly, phototaxis clearly continued throughout the treatment.

We next exposed *V. carteri* to dynamic light stimuli and fixed frequencies of electric current. At first, the behaviour was similar to that seen with continuous current; however, after 150 s, there was a large drop in the maximum number of *V. carteri* able to move back to the top of the chamber. This indicates that the fixed pulses of current hinder *V. carteri* phototaxis compared with continual exposure to electricity. The reduction in phototaxis was gradual but clear towards the end of the experiment when most *V. carteri* are distributed equally throughout each quadrant, indicating that the *V. carteri* are not localized to any particular side over time and are hence moving less.

Finally, new *V. carteri* were subjected to random pulses of current while exposed to a switching light source. Randomized current pulses interrupted phototactic behaviour much more quickly (at approximately 225 s compared with greater than 325 s for the fixed current pulses, while continuous current exposure did not exhibit a clear phototactic interruption point). Interestingly, in neurons, repetitive application of electric shock pulses can cause a progressive but reversible decrease in spontaneous depolarizing potentials [54].

Combined, these experiments show that repeated electric shocks interfere with normal *V. carteri* photoadaptation, indicating that maintenance of a constant or predictable voltage is required for the temporal fidelity of photoadaptation in *V. carteri.*

While the channelrhodopsin protein responsible for light sensing and downstream calcium flow into flagella is not directly voltage gated, a similar mechanism could affect its spontaneous ability to open in response to light, but this would need to be studied further in future studies. Furthermore, as the L-type calcium channels that facilitate signal conduction from photoreceptor to flagella are voltage gated, the application of electric shocks could also directly interfere with the temporal characteristics of photoadaptation, similar to the mode explored in §3.4.

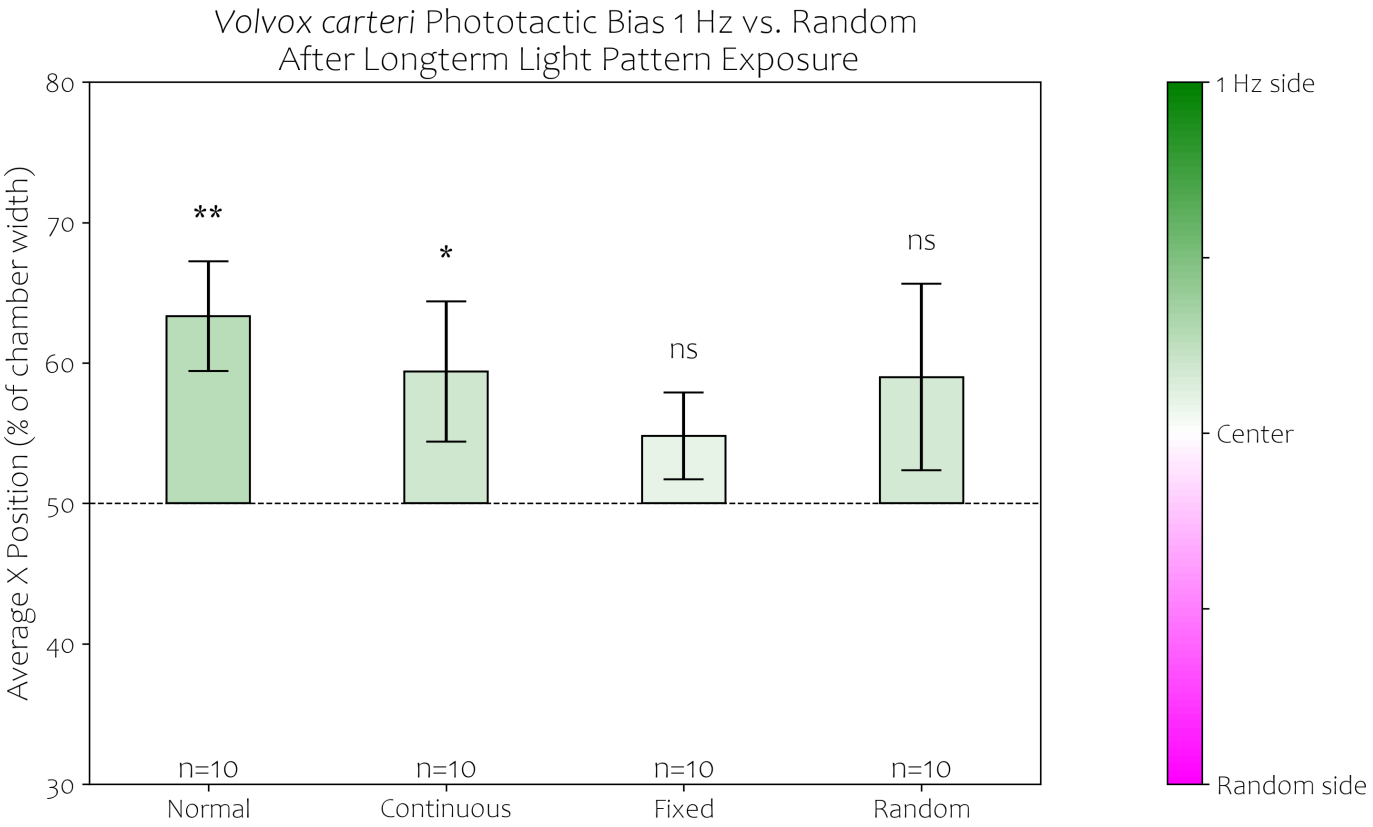

Figure 10. Long-term light pattern exposed *V. carteri* lose phototactic biases against random light stimulation. *Volvox carteri* exposed to randomized ('random') and 1 Hz ('fixed') light pulse frequency no longer exhibit a phototactic bias towards the 1 Hz stimulus side compared with control colonies in the same experimental study. This indicates a habituation to the patterned light pulse series in both cases. 'Continuous', 'fixed' and 'random' were treated in the LED dome devices described in §2.6, while the 'normal' group refers to *V. carteri* cultured under standard growth lights used for all *Volvox* cultures.

4. Discussion

Using the example of the green algae *Volvox*, we have provided a minimalistic realization of physiological equations that govern the inherent pattern recognition and surprise minimization realized by the phototaxis adaptive response. This adaptive response was shown not just to be input frequency dependent but was also capable of differentiating a more regular from an irregular input modulation. Furthermore, by employing in our experimental approach two different species of *Volvox* that are evolutionarily close to each other (approximately 75 Myr of evolutionary distance [40]), we were able to show that while small variations in phototactic preferences towards different light pulse frequencies were present, preference towards regular over irregular patterns was present in both species in our comparison of a 1 Hz light pulse series versus the randomized light pulse series, consistent with uncertainty minimization. Indeed, based on light pulse frequency alone, the lack of frequency-induced biases between 1 and 2 Hz in *V. carteri*, and a photo bias in favour of the higher 2 Hz frequency against 1 Hz in *V. aureus* would have led to the prediction that *V. carteri* would have exhibited a lack of any photo bias, and stronger photo bias towards the random stimuli in *V. aureus*, as the Poisson-distributed random stimulation light pulse series has a high proportion of short light pulse sequences of 2 Hz (see figure 6f). We note, however, that we cannot rule out other possible models of behaviour in *Volvox*, which could be formulated in the future.

The observed pharmacological and long-term light stimulation-induced shift in photo biases suggests that, while fine-tuned and probably coevolved with body rotation, the optimal frequency response is mechanistically independent and influenced by additional factors. This complexity hence extends beyond a simple, hard-wired single-frequency preference, as further evidenced by the differing optimal light pulse frequency biases between *V. carteri* and *V. aureus*. While we cannot claim that *Volvox's* ability to distinguish a regular stimulation pattern from a randomized one can operate at all possible frequencies, the ability to preferentially detect and adapt to a regular input pattern observed in two different species of *Volvox* is a surprising finding predicted by our cognitive framework. To expand our understanding of the extent of this capability, future work should examine both a broader range of frequencies and also more diverse and complex patterns to see what is possible in this aneural organism.

The significant variance across individuals that we observed for both species most likely stems from a combination of (to a lesser extent) remaining light artefacts of non-parallel illumination, and (to a higher extent) initial distribution of sizes and random starting positions. Moreover, variances between individual *Volvox* size and age (in terms of their stage in their lifecycle), health, eccentricity (how much they deviate from a perfect spherical shape that influences their tumbling and hence fidelity of their phototactic behaviour) and any possible flagellar patterning aberrations (stemming from slight deviations from ideal morphogenetic processes, which would also affect their tumbling), are all likely to introduce variations in their ability to react and move towards different light patterns as predicted. Lastly, any significant biochemical variations between *Volvox*, such as

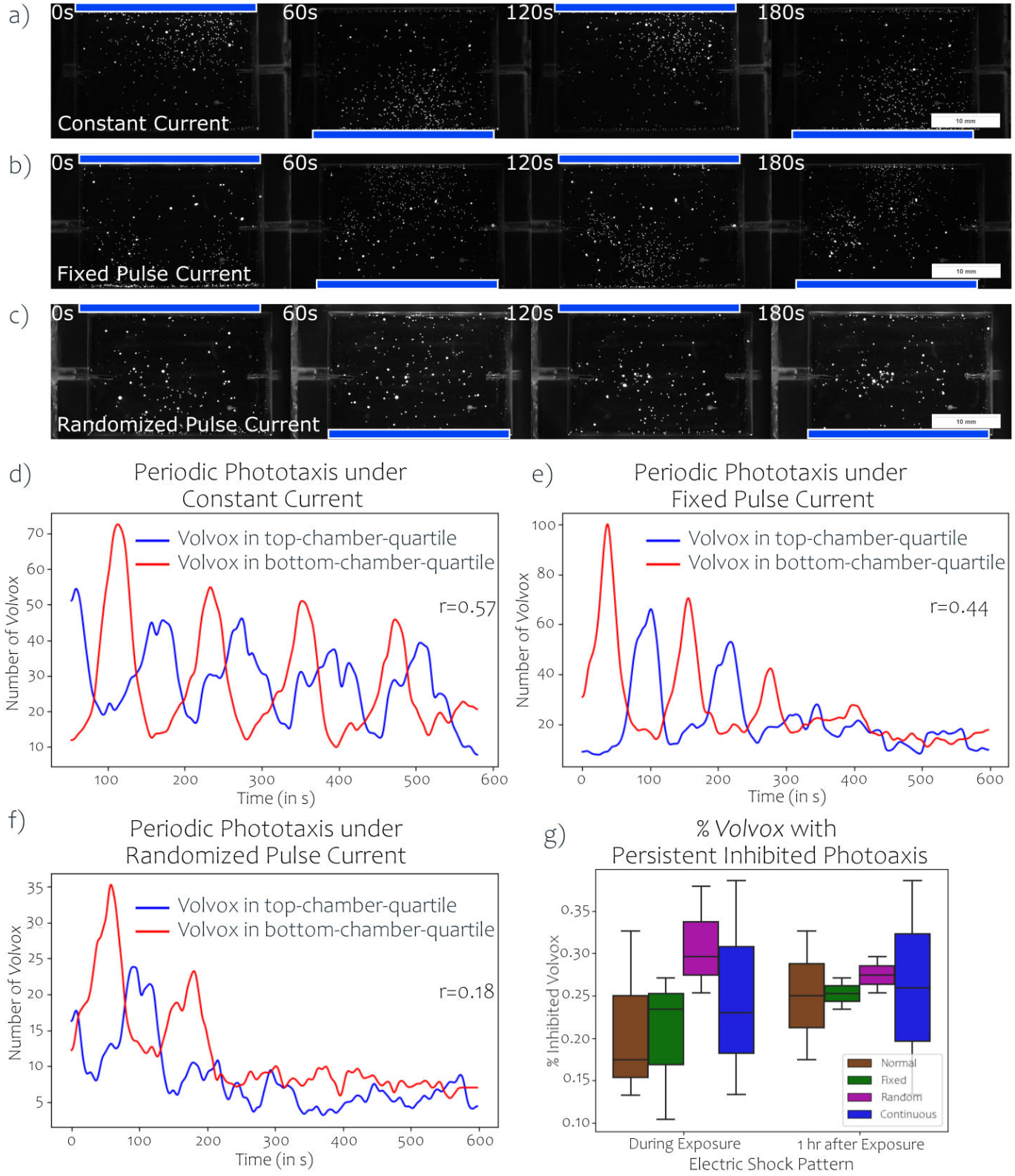

Figure 11. Pulsed electric shock inhibits adaptive phototaxis. (a–c) Montage of *V. carteri* localization following oscillating dynamic light source, under continuous (a), fixed 1 Hz (b) and randomized (c) pulse-sequenced electric shocks at 3 V. Blue bars show the light source in each time frame. (d–f) Quantification of number of *V. carteri* in each half of the chamber (blue and red lines show the number of *V. carteri* in the chamber close to the top and bottom light sources, respectively.) While photoadaptation under constant current was slightly attenuated over time, but otherwise largely intact (d), it declines sooner under a fixed shock pulse sequence (e), and even more rapidly under a randomized pulse sequence (f). (g) Effect of treatment on *V. carteri* motility. We counted the number of *V. carteri* that were no longer exhibiting any kind of motion at the end of the 30 min treatment and 1 h later in three replicates each, as an indicator of overall health and found no detectable statistically significant reduction of motility over time between any of the electric shock treatment groups (two-way ANOVA).

internal calcium storages and channelrhodopsin excitability, would also affect the speed and duration of their photoadaptive machinery and would, in turn, shift any phototactic biases as well.

By elucidating the mechanism that governs the physiological response variables through calcium in *V. carteri*, we have shown how a system is fine-tuned to certain expected signals in terms of its characteristic response and adaptive time constants setting the perception limits of individual stimulation pulses. Based on abstract uncertainty minimization alone without any

mechanistic underpinning alone, we would have predicted that nimodipine should not change the preference to a patterned versus a randomized input; however, that bias is probably substantially hidden here because of the modulation of frequency response by nimodipine. This is analogous to the reason that white noise does not illicit a strong aversion or stress response in humans unless at high decibels: despite its highly random nature, the randomly distributed frequencies are too high to be perceived by human brains as individual pulses, but instead blend together as a background that can even be soothing to infants [55], or help with concentration by tuning out more perceivable randomly occurring acoustic events in the environment [56]. Future work could endeavour to truly, quantitatively map out the variational free energy minimization dynamics of photoadaptation by conducting time-lapse experiments on the electrical dynamics (such as through fluorescent voltage or calcium reporters) and perform dynamic causal modelling (DCM) on the resulting time series to infer underlying Bayesian models of photoadaptation in *V. carteri*. In neuroscience, the employment of DCMs on functional data such as functional magnetic resonance imaging (fMRI) data allows experimental data-driven estimation of effective connectivity among brain regions based on differential equations constructed through mechanistic insights of neuronal activity and indicate causal interactions that produce task-driven behaviour. Constructing DCMs with more detailed mechanistic insights into *Volvox* photoadaptation hence has the potential to construct and test models of *Volvox* behaviour more generally and at a higher level than that which our current knowledge allows. In addition to specific mechanistic insight into photoadaptation in *V. carteri*, these findings will provide insight into how the minimization of variational free energy at the root of surprise minimization [23] is implemented mechanistically in an organism with a simple behaviour, equipping us with the knowledge and tools needed to look for similar behavioural modes in other systems and to manipulate them [57,58].

We also showed that the direct metabolic function of *V. carteri* in terms of photosynthetic output appears to be largely unaffected by light pattern recognition through the observed phototactic biases observed throughout this work, as the patterned light treatment groups did not show statistically significant decreases in oxygen concentration within the statistical power and temporal precision of this experiment. Any trend that we saw here in terms of slightly lower oxygen concentration in the random group would have to be extended in future experiments under longer time frames that carefully observe and control for differences in colony and population growth that could be obscuring those trends in our current results. Higher precision oxygen measurements or live reporters of metabolic activity would also have the potential to determine whether short-term photoadaptation in response to different light patterns as observed in our phototactic experiments is accompanied by immediate metabolic differences. As it stands, this is evidence supporting the notion that any long-term adaptive response by *V. carteri* to light patterns is also not driven by a purely energy-based selection pressure. While evolutionary principles inevitably apply here too, the selection pressure would appear to be more nuanced than simply a question of which light pattern yields the highest photosynthetic yield. While long-term experiments measuring the effect of other flashing light frequencies on *Volvox* growth have not been carried out, research on the microalgae *Chlorella vulgaris* provides evidence in support of our conclusion, where no difference in growth rate, absolute pigment composition and light curve characteristics have been observed at frequencies of 1 Hz and higher compared with equal amount of continuous light, but lower growth rates were observed at 0.1 Hz [59]. These two findings together support our conclusion that modes of photoadaptation occur at different, independent frequencies with respect to photosynthesis and phototaxis.

Future work could more explicitly investigate whether it is possible to introduce strong biases in phototaxis towards a more predictable pattern that, however, yields lower photosynthetic outcomes, which would be evidence for proto-cognitive/informational considerations overriding metabolic imperatives. This would support the argument that informational concerns need to be more explicitly addressed in evolutionary approaches [30,34].

Throughout this work, we referred to the short-term changes in light sensitivity in the eyespot and downstream flagellar beating responsivity in *V. carteri* that are the core of their ability to orient themselves towards light and maintain direction as *photoadaptation*, as in previous studies [18]. This notation aligns well with how adaptation is used in neuroscience, specifically when referring to the visual system. Short-term processes like visual reduction or increase of light sensitivity to changing light conditions are referred to as adaptive [60]. Indeed, short-term synaptic depression, which is very similar to what we observe here, is the central part of these adaptive responses [61] and is the precursor to long-term depression (LTD) that underlies learning in neural systems together with its opposite, long-term potentiation (LTP).

Interestingly, although constant-frequency stimulation trains are the standard stimulation method for many experimental studies on synaptic plasticity, they are unlikely to be experienced by neurons in a real brain, where inputs tend to be much more irregular [42]. In fact, the Poisson distribution that best describes our randomized light pulse stimulation is also one of the most representative stimulation patterns in brains *in vivo* [42]. Given the common evolutionary ancestry of the voltage-gated ion channels in neurons and the light-gated ion channels controlling flagellar motion in *V. carteri*, we considered how the inter-light pulse dependency of photoadaptation in *V. carteri* may be related to STDP in neurons. STDP refers to the finding that the sign and magnitude of changes in neuronal synaptic strength (a foundation of learning in neural networks) depend on the precise timing of action potential spikes in the stimulus [43].

Additional parallels to the calcium-mediated response in *V. carteri* may be indicated by the fact that synaptic signal transmission is also highly modulated by dynamic calcium fluxes. In addition to its dependence on stimulus timing, Hata *et al.* examined, *in silico*, the critical role of post-synaptic Ca^{2+} flux in synaptic modulation [42]. Changing the post-synaptic neuron's calcium decay constant from 40 to 80 ms switches the effect of stimulation with Poisson-distributed activity between the two most fundamental changes to synaptic strength that underlie all learning processes, LTD and LTP. When the postsynaptic neuron's calcium decay constant is 80 ms, the stimulus results in long-term potentiation; if it is 40 ms, the same stimulus results in long-term depression [42]. Hata *et al.* also showed that postsynaptic calcium levels were reduced for Poisson-distributed inter-spike distances compared with fixed frequency spike trains. This finding is particularly relevant to the photoresponse in *V. carteri*, as its calcium-dependent ion channels propagate the response from the photoreceptor (which is channelrhodopsin

mediated) to the flagellum, downregulating flagellar beating frequency and hence determining fluid speed on the *V. carteri* colony surface [48]. Calcium activity in the *V. carteri* photoresponse is largely dependent on two time scales: the initiation of a calcium current is of the order of 1 ms, while the diffusion of calcium along the flagellum is of the order of 200 ms [18].

In addition, we have proven the existence of basic memory in phototactic alignment in *V. aureus* as a necessary condition for pattern recognition and temporal stimulus tracking. By persisting on phototactic trajectories set in past light stimuli, *V. aureus* have at least one of two major necessary components for learning: memory and plasticity. One can speculate that this behaviour evolved to maintain phototactic orientation when momentarily exposed to shadows, which would be a very clear illustration of why memory and learning could evolve even in such low complexity organisms. Indeed, research by Mast showed that upon a drastic decrease in light stimulus, *Volvox* exhibit reduced rotational speed and hence faster forward movement [62], thereby stabilizing directed movement towards the light during short periods of light obstruction.

Finally, we have shown that *V. carteri* can adapt over time to light patterns that they seem to avoid due to their unpredictability, laying the groundwork for studying the evolution of specific, temporally fine-tuned adaptive responses in simple organisms with the promise to advance current undertakings in biomedicine, exobiology and synthetic morphoengineering [57,63]. This finding also suggests that *V. carteri* exhibit plasticity in their behaviour in response to the information content of their environment, as represented by the pattern recognition mode we tested throughout this work. While detailed molecular analyses (to study possible differences in the accumulation of mutations, changes in transcriptional state changes and protein compositions) and possibly cell lineage tracing (to determine the role of variable growth patterns in this long-term adaptation) need to be performed on the make-up of these phototactic changes in future work, this is a clear indication that pattern recognition can lead to long-term changes in aneural organism and even potentially be a drive for evolutionary change as we have previously hypothesized [30]. In molecularly tractable living systems, assays based on the concepts of this article offer the possibility of understanding memory, learning and intelligence across a very wide range of substrates [64–69]. The fully annotated genome of *V. carteri* will allow us to examine transcriptional responses as part of the photoadaptive response. For example, through ubiquitous cellular stress response pathways, such as heat shock proteins, we could test whether unsuccessful uncertainty minimization (in response to the randomized stimuli in our experiments) would be accompanied by higher amounts of stress in algae in a similar manner as observed in humans [53].

5. Conclusions

The aim of this study was to provide an experimental example of a general behavioural directive in terms of uncertainty minimization that spans aneural and neural organisms. We have shown through the phototactic biases observed in *Volvox* towards more regular light pulse patterns, and our extensive manipulations thereof, how irregular, unpredictable signalling activation leads to a reduced capability of simple cognitive systems to detect and distinguish regular from random patterns, as predicted by variational free energy minimization, and hence correctly infer and perform correct action–perception, thereby successfully applying this neurocentric behavioural directive to an aneural organism.

Our results show that *Volvox's* photoadaptive behaviour exhibits a crucial component of basal intelligence: the ability to recognize patterns in input stimuli. In combination with simulations of the photoadaptive mechanisms in *Volvox* and pairing the light stimuli with photocurrent altering drugs and electric shocks, we showed how the randomized light pulses and electric shocks interfere with normal photoadaptation as a consequence of a structured dynamic interplay with colony rotation and the information transfer from photoreceptor to flagellar deactivation that encodes for what we determine to be an example of uncertainty minimization. The ability of algae to be surprised and distinguish random events that do not meet expected patterns, as well as the additional finding of memory in *Volvox* in terms of persistence of movement towards past light stimulation further expands concepts such as uncertainty minimization and stimulus generalization beyond neurons.

It should be noted that our use of the uncertainty minimization framework to discover the response described herein is not incompatible with molecular-level descriptions of the events that implement it. Just as in neuroscience, a complete explanation will probably involve both—high-level principles that efficiently enable the discovery of new behavioural models and low-level molecular details of implementation that are consistent with the decision-making algorithms observed and exploited by evolution, by other life forms in the environment, and by bioengineers [70].

In future work, the bridging between physiological differential equations governing adaptive responses and information processing, predictive-coding-based approaches such as the free energy principle needs to be made explicit into one combined framework. Fundamentally, the ability to distinguish regular versus random stimuli requires the agent to detect a pattern, which, in turn, can be used as a kind of IQ test; how complex of a pattern can *Volvox* (or any other unconventional model system) detect and distinguish from randomness? This will be determined in future work. Such assays, in molecularly tractable living systems, offer the possibility of understanding memory, learning and intelligence across a very wide range of substrates—a possibility that may have considerable implications for biomedicine, exobiology and synthetic morphoengineering.

Equipped with explicit, mechanistic implementations of surprise minimization, it may be possible to achieve much improved rational control over cellular function and organismal behaviour that would not necessitate rewriting the internal model of a cell (such as its DNA through gene therapy). Instead, it would rely on managing spatio-temporal control of the environmental signals an organism receives, building on many recent biotechnological breakthroughs, such as optogenetics, to study and take advantage of the many unexpected competencies of biological materials.

Ethics. This work did not require ethical approval from a human subject or animal welfare committee.

Data accessibility. We have attached a zip file (as electronic supplementary material), which contains data from our research for this paper. We have also attached, as electronic supplementary material, a data description file containing descriptive titles and descriptions for each of the files in that zip file. The code and data that fully generates the graphs from the figures can be found at Zenodo [71].

Supplementary material is available online [72].

Declaration of AI use. We have not used AI-assisted technologies in creating this article.

Authors' contributions. F.K.: conceptualization, data curation, formal analysis, investigation, methodology, software, supervision, visualization, writing—original draft, writing—review and editing; I.S.: formal analysis, investigation, methodology, visualization, writing—original draft; M.D.: investigation; S.Z.: investigation; A.K.: investigation; M.L.: conceptualization, funding acquisition, funding acquisition, project administration, project administration, supervision, supervision, writing—review and editing, writing—review and editing.

All authors gave final approval for publication and agreed to be held accountable for the work performed therein.

Conflict of interest declaration. We declare we have no competing interests.

Funding. M.L. gratefully acknowledges support via grant 62212 from the John Templeton Foundation. The opinions expressed in this publication are those of the author(s) and do not necessarily reflect the views of the John Templeton Foundation.

Acknowledgements. We thank the Olson Lab, Bradley Olson and Berenice Jiménez-Marín in particular, for providing the *V. carteri* strains and guidance on culture maintenance. We also thank Dimitri Kromm, Juanita Mathews and Wesley Clawson for their comments on this manuscript and, together with Devon Davidian, for helpful discussions and advice on experimental techniques. We also thank Karl Friston for his guidance and scientific body of work that inspired the approach in this manuscript. We are very grateful to Eugene Jhong for the support that facilitated this work. We thank Susan Lewis and Julia Poirier for their invaluable help with manuscript editing and preparation.

References

1. Baluška F, Levin M. 2016 On having no head: cognition throughout biological systems. *Front. Psychol.* **7**, 902. (doi:10.3389/fpsyg.2016.00902)
2. Lyon P. 2006 The biogenic approach to cognition. *Cogn. Process.* **7**, 11–29. (doi:10.1007/s10339-005-0016-8)
3. Lyon P. 2015 The cognitive cell: bacterial behavior reconsidered. *Front. Microbiol.* **6**, 264. (doi:10.3389/fmicb.2015.00264)
4. Jennings HS. 1931 *Behavior of the lower organisms*. New York, NY: Columbia University Press.
5. Losick RM. 2020 *Bacillus subtilis*: a bacterium for all seasons. *Curr. Biol.* **30**, R1146–R1150. (doi:10.1016/j.cub.2020.06.083)
6. Thiery S, Kaimer C. 2020 The predation strategy of *Myxococcus xanthus*. *Front. Microbiol.* **11**, 2. (doi:10.3389/fmicb.2020.00002)
7. Wolf DM, Fontaine-Bodin L, Bischofs I, Price G, Keasling J, Arkin AP. 2008 Memory in microbes: quantifying history-dependent behavior in a bacterium. *PLoS One* **3**, e1700. (doi:10.1371/journal.pone.0001700)
8. Tagkopoulos I, Liu YC, Tavazoie S. 2008 Predictive behavior within microbial genetic networks. *Science* **320**, 1313–1317. (doi:10.1126/science.1154456)
9. Murugan NJ *et al*. 2021 Mechanosensation mediates long-range spatial decision-making in an aneural organism. *Adv. Mater. Weinheim* **33**, e2008161. (doi:10.1002/adma.202008161)
10. Shirakawa T, Gunji YP, Miyake Y. 2011 An associative learning experiment using the plasmodium of *Physarum polycephalum*. *Nano Commun. Netw.* **2**, 99–105. (doi:10.1016/j.nancom.2011.05.002)
11. Allan C, Morris RJ, Meisrimler CN. 2022 Encoding, transmission, decoding, and specificity of calcium signals in plants. *J. Exp. Bot.* **73**, 3372–3385. (doi:10.1093/jxb/erac105)
12. Baluška F, Mancuso S. 2021 Individuality, self and sociality of vascular plants. *Phil. Trans. R. Soc. B* **376**, 20190760. (doi:10.1098/rstb.2019.0760)
13. Beilby MJ. 2007 Action potential in charophytes. *Int. Rev. Cytol.* **257**, 43–82. (doi:10.1016/S0074-7696(07)57002-6)
14. Appel HM, Cocroft RB. 2014 Plants respond to leaf vibrations caused by insect herbivore chewing. *Oecologia* **175**, 1257–1266. (doi:10.1007/s00442-014-2995-6)
15. Wang H, Tao Y, Li Y, Wu S, Li D, Liu X, Han Y, Manickam S, Show PL. 2021 Application of ultrasonication at different microbial growth stages during apple juice fermentation by *Lactobacillus plantarum*: investigation on the metabolic response. *Ultrason. Sonochemistry* **73**, 105486. (doi:10.1016/j.ultsonch.2021.105486)
16. Godfrey-Smith P. 2020 *Metazoa: animal life and the birth of the mind*. New York, NY: Farrar, Straus and Giroux.
17. Deacon TW. 2011 *Incomplete nature: how mind emerged from matter*. New York, NY: WW Norton & Company.
18. Drescher K, Goldstein RE, Tuval I. 2010 Fidelity of adaptive phototaxis. *Proc. Natl Acad. Sci. USA* **107**, 11171–11176. (doi:10.1073/pnas.1000901107)
19. Mitchell A, Wei P, Lim WA. 2015 Oscillatory stress stimulation uncovers an Achilles' heel of the yeast MAPK signaling network. *Science* **350**, 1379–1383. (doi:10.1126/science.aab0892)
20. Bugaj LJ, O'Donoghue GP, Lim WA. 2017 Interrogating cellular perception and decision making with optogenetic tools. *J. Cell Biol.* **216**, 25–28. (doi:10.1083/jcb.201612094)
21. Toettcher JE, Weiner OD, Lim WA. 2013 Using optogenetics to interrogate the dynamic control of signal transmission by the Ras/Erk module. *Cell* **155**, 1422–1434. (doi:10.1016/j.cell.2013.11.004)
22. Wilson MZ, Ravindran PT, Lim WA, Toettcher JE. 2017 Tracing information flow from Erk to target gene induction reveals mechanisms of dynamic and combinatorial control. *Mol. Cell* **67**, 757–769. (doi:10.1016/j.molcel.2017.07.016)
23. Kuchling F, Friston K, Georgiev G, Levin M. 2019 Morphogenesis as Bayesian inference: a variational approach to pattern formation and control in complex biological systems. *Phys. Life Rev.* **33**, 88–108. (doi:10.1016/j.plrev.2019.06.001)
24. Pezzulo G, Cartoni E, Rigoli F, Pio-Lopez L, Friston K. 2016 Active Inference, epistemic value, and vicarious trial and error. *Learn. Mem.* **23**, 322–338. (doi:10.1101/lm.041780.116)
25. Friston K. 2013 Life as we know it. *J. R. Soc. Interface* **10**, 20130475. (doi:10.1098/rsif.2013.0475)
26. Pezzulo G, Parr T, Friston K. 2022 The evolution of brain architectures for predictive coding and active inference. *Phil. Trans. R. Soc. B* **377**, 20200531. (doi:10.1098/rstb.2020.0531)
27. Friston K, Levin M, Sengupta B, Pezzulo G. 2015 Knowing one's place: a free-energy approach to pattern regulation. *J. R. Soc. Interface* **12**, 20141383. (doi:10.1098/rsif.2014.1383)
28. Chater N, Oaksford M, Hahn U, Heit E. 2010 Bayesian models of cognition. *WIRES Cognitive Science* **1**, 811–823. (doi:10.1002/wcs.79)
29. Colas F, Diard J, Bessière P. 2010 Common Bayesian models for common cognitive issues. *Acta Biotheor.* **58**, 191–216. (doi:10.1007/s10441-010-9101-1)
30. Kuchling F, Fields C, Levin M. 2022 Metacognition as a consequence of competing evolutionary time scales. *Entropy (Basel)* **24**, 601. (doi:10.3390/e24050601)
31. Lyon P, Kuchling F. 2021 Valuing what happens: a biogenic approach to valence and (potentially) affect. Phil. Trans. R. Soc. B **376**, 20190752. (doi:10.1098/rstb.2019.0752)
32. Karl F. 2012 A free energy principle for biological systems. *Entropy (Basel)* **14**, 2100–2121. (doi:10.3390/e14112100)
33. Kirchhoff M, Parr T, Palacios E, Friston K, Kiverstein J. 2018 The Markov blankets of life: autonomy, active inference and the free energy principle. *J. R. Soc. Interface* **15**, 20170792. (doi:10.1098/rsif.2017.0792)

34. Campbell JO. 2016 Universal Darwinism as a process of Bayesian inference. *Front. Syst. Neurosci.* **10**, 49. (doi:10.3389/fnsys.2016.00049)
35. Keijzer F, van Duijn M, Lyon P. 2013 What nervous systems do: early evolution, input–output, and the skin brain thesis. *Adapt. Behav.* **21**, 67–85. (doi:10.1177/1059712312465330)
36. Fields C, Bischof J, Levin M. 2020 Morphological coordination: a common ancestral function unifying neural and non-neural signaling. *Physiology* **35**, 16–30. (doi:10.1152/physiol.00027.2019)
37. Jiménez-Marín B, Rakijas JB, Tyagi A, Pandey A, Hanschen ER, Anderson J, Heffel MG, Platt TG, Olson BJSC. 2023 Gene loss during a transition to multicellularity. *Sci. Rep.* **13**. (doi:10.1038/s41598-023-29742-2)
38. Frank TD. 2012 Multistable pattern formation systems: candidates for physical intelligence? *Ecol. Psychol.* **24**, 220–240. (doi:10.1080/10407413.2012.702626)
39. Stasenko S, Telnykh A, Shemagina O, Nuidel I, Kovalchuk A, Yakhno V. 2022 Biomorphic artificial intelligence system for pattern recognition problems with adaptive error correction. In *2022 4th Int. Conf. Neurotechnologies and Neurointerfaces (CNN)*, Kaliningrad, Russian Federation, pp. 185–189. IEEE. (doi:10.1109/CNN56452.2022.9912537)
40. Herron MD. 2016 Origins of multicellular complexity: *Volvox* and the volvocine algae. *Mol. Ecol.* **25**, 1213–1223. (doi:10.1111/mec.13551)
41. Solari CA, Drescher K, Ganguly S, Kessler JO, Michod RE, Goldstein RE. 2011 Flagellar phenotypic plasticity in volvocalean algae correlates with Péclet number. *J. R. Soc. Interface* **8**, 1409–1417. (doi:10.1098/rsif.2011.0023)
42. Hata K, Araki O, Yokoi O, Kusakabe T, Yamamoto Y, Ito S, Nikuni T. 2020 Multicoding in neural information transfer suggested by mathematical analysis of the frequency-dependent synaptic plasticity in vivo. *Sci. Rep.* **10**, 13974. (doi:10.1038/s41598-020-70876-4)
43. Shouval HZ, Wang SS, Wittenberg GM. 2010 Spike timing dependent plasticity: a consequence of more fundamental learning rules. *Front. Comput. Neurosci.* **4**, 19. (doi:10.3389/fncom.2010.00019)
44. Amarasingham A, Chen TL, Geman S, Harrison MT, Sheinberg DL. 2006 Spike count reliability and the Poisson hypothesis. *J. Neurosci.* **26**, 801–809. (doi:10.1523/JNEUROSCI.2948-05.2006)
45. Wiener MC, Richmond BJ. 2003 Decoding spike trains instant by instant using order statistics and the mixture-of-Poissons model. *J. Neurosci.* **23**, 2394–2406. (doi:10.1523/JNEUROSCI.23-06-02394.2003)
46. Leptos KC, Chioccioli M, Furlan S, Pesci AI, Goldstein RE. 2023 Phototaxis of *Chlamydomonas* arises from a tuned adaptive photoresponse shared with multicellular Volvocine green algae. *Phys. Rev. E* **107**, 014404. (doi:10.1103/PhysRevE.107.014404)
47. de Maleprade H, Moisy F, Ishikawa T, Goldstein RE. 2020 Motility and phototaxis of *Gonium*, the simplest differentiated colonial alga. *Phys. Rev. E* **101**. (doi:10.1103/PhysRevE.101.022416)
48. Braun FJ, Hegemann P. 1999 Two light-activated conductances in the eye of the green alga *Volvox carteri*. *Biophys. J.* **76**, 1668–1678. (doi:10.1016/S0006-3495(99)77326-1)
49. Nelson MT, Worley JF. 1989 Dihydropyridine inhibition of single calcium channels and contraction in rabbit mesenteric artery depends on voltage. *J. Physiol.* **412**, 65–91. (doi:10.1113/jphysiol.1989.sp017604)
50. Akaike N, Kostyuk PG, Osipchuk YV. 1989 Dihydropyridine-sensitive low-threshold calcium channels in isolated rat hypothalamic neurones. *J. Physiol* **412**, 181–195. (doi:10.1113/jphysiol.1989.sp017610)
51. Hegemann P, Neumeier K, Hegemann U, Kuehnle E. 1990 The role of calcium in *Chlamydomonas* photomovement responses as analysed by calcium channel inhibitors. *Photochem. Photobiol.* **52**, 575–583. (doi:10.1111/j.1751-1097.1990.tb01802.x)
52. Supple JA, Varennes-Phillit L, Gajjar-Reid D, Cerkvenik U, Belušič G, Krapp HG. 2022 Generating spatiotemporal patterns of linearly polarised light at high frame rates for insect vision research. *J. Exp. Biol.* **225**. (doi:10.1242/jeb.244087)
53. de Berker AO, Rutledge RB, Mathys C, Marshall L, Cross GF, Dolan RJ, Bestmann S. 2016 Computations of uncertainty mediate acute stress responses in humans. *Nat. Commun.* **7**, 10996. (doi:10.1038/ncomms10996)
54. Calabresi P, Mercuri NB, Stefani A, Bernardi G. 1990 Synaptic and intrinsic control of membrane excitability of neostriatal neurons. I. An in vivo analysis. *J. Neurophysiol.* **63**, 651–662. (doi:10.1152/jn.1990.63.4.651)
55. Karakoç A, Türker F. 2014 Effects of white noise and holding on pain perception in newborns. *Pain Manag. Nurs.* **15**, 864–870. (doi:10.1016/j.pmn.2014.01.002)
56. Awada M, Becerik-Gerber B, Lucas G, Roll S. 2022 Cognitive performance, creativity and stress levels of neurotypical young adults under different white noise levels. *Sci. Rep.* **12**, 14566. (doi:10.1038/s41598-022-18862-w)
57. Davies J, Levin M. 2023 Synthetic morphology with agential materials. *Nat. Rev. Bioeng* **1**, 46–59. (doi:10.31219/osf.io/xrv8h)
58. Pezzulo G, Levin M. 2015 Re-membering the body: applications of computational neuroscience to the top-down control of regeneration of limbs and other complex organs. *Integr. Biol. (Camb)* **7**, 1487–1517. (doi:10.1039/c5ib00221d)
59. Levasseur W, Perré P, Pozzobon V. 2023 *Chlorella vulgaris* acclimated cultivation under flashing light: an in-depth investigation under iso-actinic conditions. *Algal Res.* **70**, 102976. (doi:10.1016/j.algal.2023.102976)
60. Kohn A. 2007 Visual adaptation: physiology, mechanisms, and functional benefits. *J. Neurophysiol.* **97**, 3155–3164. (doi:10.1152/jn.00086.2007)
61. Chance FS, Nelson SB, Abbott LF. 1998 Synaptic depression and the temporal response characteristics of V1 cells. *J. Neurosci.* **18**, 4785–4799. (doi:10.1523/JNEUROSCI.18-12-04785.1998)
62. Mast SO. 1926 Reactions to light in *Volvox*, with special reference to the process of orientation. *Z. f. Vergl. Physiologie* **4**, 637–658. (doi:10.1007/BF00342378)
63. Lagasse E, Levin M. 2023 Future medicine: from molecular pathways to the collective intelligence of the body. *Trends Mol. Med.* **29**, 687–710. (doi:10.1016/j.molmed.2023.06.007)
64. Katz Y, Fontana W. 2022 Probabilistic inference with polymerizing biochemical circuits. *Entropy (Basel)* **24**, 629. (doi:10.3390/e24050629)
65. Katz Y, Springer M, Fontana W. 2018 Embodying probabilistic inference in biochemical circuits. *arXiv*. (doi:10.48550/arXiv.1806.10161)
66. Katz Y, Goodman ND, Kersting K, Kemp C, Tenenbaum JB. 2008 Modeling semantic cognition as logical dimensionality reduction. In *Proc. of 30th Annual Conf. of the Cognitive Science Society*. Austin, TX: Cognitive Science Society.
67. Katz Y, Springer M. 2016 Probabilistic adaptation in changing microbial environments. *PeerJ* **4**, e2716. (doi:10.7717/peerj.2716)
68. Biswas S, Clawson W, Levin M. 2022 Learning in transcriptional network models: computational discovery of pathway-level memory and effective interventions. *Int. J. Mol. Sci.* **24**. (doi:10.3390/ijms24010285)
69. Biswas S, Manicka S, Hoel E, Levin M. 2021 Gene regulatory networks exhibit several kinds of memory: quantification of memory in biological and random transcriptional networks. *iScience* **24**, 102131. (doi:10.1016/j.isci.2021.102131)
70. Marr D. 2010 *Vision: a computational investigation into the human representation and processing of visual information*. Cambridge, MA: MIT Press.
71. Kuchling F. 2025 Data from: Uncertainty Minimization and Pattern Recognition in *V. Carteri* and *V. Aureus*. Zenodo. (doi:10.5281/zenodo.14656457)
72. Kuchling F, Singh I, Daga M, Zec S, Kunen A, Levin M. 2025 Supplementary material from: Uncertainty Minimization and Pattern Recognition in *V. carteri* and *V. aureus*. Figshare. (doi:10.6084/m9.figshare.c.7681862)